Musculoskeletal system simulations to analyse muscle forces and movement pattern

by

Markus Stålbom

December 2008
Master Thesis from
Royal Institute of Technology
Department of Mechanics
SE-100 44 Stockholm, Sweden

Abstract

The musculoskeletal system of the human is a complex system that still has a lot of unsolved mysteries. There is plenty of research being performed right at this moment which is trying to better understand the movement apparatus of the human. In spite of all research being conducted, there are no clear description of the important issues of which facts determine how much and which muscle activates in different movements. This also raises the question of the amount of force each muscle contributes with over the different joints for different movements.

The aim of the thesis was to develop a musculotendon unit model for use in optimal control simulations. The model was targeting to be specialized to handle optimization problems in stretch-shortening sport movements.

The work was concentred on the development of a musculotendon (MT) -unit model, consisting of the muscle and its belonging tendon structure. The model included features for force-velocity and force-length relationship, elasticity of cross-bridges and the passive structures in muscles. The model was made dimensionless which opened the possibility to use it for all skeletal muscles in the body together with the muscle specific parameters. Excluded in the model was the possibility of variable muscle activity and pennation angle.

The purpose of the MT-unit model was to incorporate it into a musculoskeletal (MS) model. The MS model developed and used consisted of one degree of freedom, two segments and one muscle. This model was then used in a drop jump simulation where the ground contact phase was evaluated. The muscle was assumed to be fully activated during the whole ground contact. This simulation generated realistic results.

Acknowledgement

This master thesis has brought me a major understanding of the human movement pattern. Understanding the human movement is in itself very interesting but trying to exactly describe why that specific movement was performed is one of my main passions.

I want to thank an old mentor and friend, Matiu Taingahue, for being the single most important person responsible for giving me the opportunities to develop my interest in human movement and biomechanics.

At the Department of Mechanics, KTH, I found a new family with peoples sharing the same interest. The person shining with the same spark as me when discussing the subject was Lanie Gutierrez and she contributed with both information and inspiration. My supervisor during this thesis was Professor Anders Eriksson contributing with experience and endless of knowledge of the difficult mathematics. He also guided me through the whole thesis, both with the day to day difficulties and the more long term problems.

Finally, my two PhD roommates at the department, Robert and Mattias, have made my thesis work much more enjoyable. Thanks for the help, support and socialization.

Table of contents

1 Introduction

The musculoskeletal system of the human is a complex system that still has a lot of unsolved mysteries. There is plenty of research being performed right at this moment which is trying to better understand the movement apparatus of the human. In spite of all research being conducted, there are no clear description of the important issues of which facts determine how much and which muscle activates in different movements. This also raises the question of the amount of force each muscle contributes over the different joints for different movements. The answers to these questions would be of great interest for a lot of professions and peoples. Professions that would be interested of this knowledge are personal trainers, gym instructors, conditioning trainers, elite actives, surgeons, physiotherapists, sport biomechanists and coaches.

Even though the picture of how muscles activate and which forces are produced is not totally clear the research has discovered many important findings. These findings, and methods of how to investigate these questions, are presented in chapter 3.

At the start of this thesis the knowledge of the field were insufficient and a large amount of energy had to be put into understanding what has been done and what is the most important questions in the field. An aim with research is to generate new findings but that require a great knowledge of previous and present work.

The author has a great interest in sports and the human movement pattern. Due to these interests many questions were posed before the thesis. Is it possible to mathematically simulate an injury and investigate the consequences on the movement pattern? If it is possible, then it could be of great value for deciding when an athlete is recovered from an injury. What kind of running technique is the most economic and which one is the best for sprinting? Is it possible to answer these questions by doing computational simulations, and in that case; which one?

Enjoy reading!

1.1 Biomechanics

The domain of interest of biomechanics is huge: it ranges across physiology (with a special focus on the musculoskeletal, cardiovascular, respiratory, and digestive apparatuses), pathology (orthopaedics and traumatology, maxillofacial surgery, dentistry and orthodontistry, cardiovascular and respiratory surgery), forensics (accident reconstructions, crime scene investigation), vehicle safety (car safety, helmets), ergonomics and workplace safety, defence and social security (combat and law enforcement protection, effectiveness of projectile weapons), and sport (performance optimization, protection devices). (Viceconti, Testi et al. 2006)

Its main scientific journal, the Journal of Biomechanics, was founded only in 1968; even later, the International Society of Biomechanics was founded in 1973, the European Society of Biomechanics in 1976, and the American Society of Biomechanics in 1977. While the research activity over these 30 years has been intense, the impact of biomechanics today is not yet as great as one may have expected. One of the main factors limiting the application of biomechanics results is that, to answer most practical questions, a global model is required (Viceconti, Testi et al. 2006).

1.2 Aim

The aim of the thesis was to develop a musculotendon unit model for use in optimal control simulations. The model was targeting to be specialized to handle optimization problems in stretch-shortening sport movements.

1.3 Objectives

- Develop a two-dimensional musculoskeletal model
- Improve the developed model according to the latest research on SSC
- Validate the model

2 Biomechanics of the human

The knowledge of the human physiology and especially the human biomechanics is of great importance when trying to model the human musculoskeletal system. The general descriptions in this chapter are relatively sparse and more focus has been placed on specific properties important for this thesis. This chapter is divided into three parts; bone and joints, skeletal musculotendon units, and stretch-shortening cycle.

2.1 Bones and joints

The skeleton in the body consists of bone connected with joints for ability to move. Bone is a hard material which gives the skeleton very good mechanical properties (Marieb 2004).

The anatomical structure of a given joint, as well as the direction of which the attached body segments are permitted to move at the joint, have very small variations from person to person. However, differences in relative tightness or laxity of the surrounding soft tissues result in different range of movement (ROM). (Hall 2003)

2.2 Skeletal musculotendon units

The structure of the human skeletal musculotendon unit is well examined and consists of the muscle and tendon. The tendons consist of collagen and elastin and connect the muscle with the bone. The muscle is divided into smaller and smaller portions starting with the whole muscle, fascicles, fibres and finally fibrils. The fibrils are built up by sarcomeres, shown in Figure 1, which consists of actin, myosin and elastic filaments. The movement of the muscle is due to the active movement between actin and myosin filaments and the elastic filament contributes to the elasticity of the muscle. (Marieb 2004).

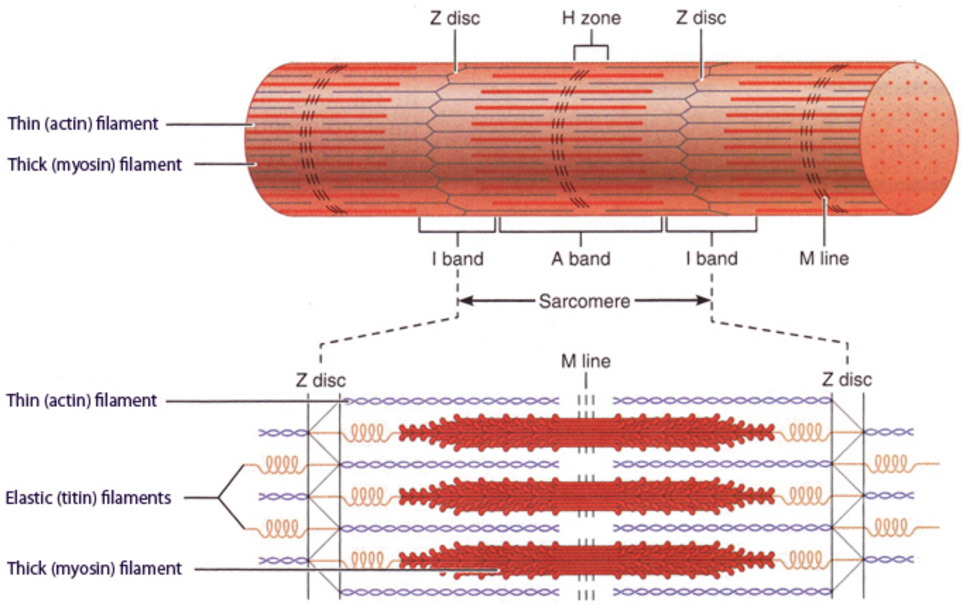

Figure 1: The myofibril (upper) and a sarcomere (lower) of a skeletal muscle. Reproduced from Marieb (2004)

2.3 Stretch-shortening cycle

An eccentric muscle action is defined as a muscle action performed during lengthening (or stretching) of the muscle and a concentric muscle action is defined as a muscle action during its shortening. The combination of an eccentric directly followed by a concentric action forms a natural type of muscle function called stretch-shortening cycle (Komi 2000). This function, or phenomenon, is present in daily life activities as walking, running and jumping. Many studies have proved that the enhancement gained from SSC mainly is due to stored elastic energy (Komi 2000).

The literature has described many factors that influence SSC in different ways. The amount of activation of the muscle before impact, called *pre-activation*, has been stated to be important (Komi 2000). Further, the change of length of the muscle fascicle compared to the tendon structure during the functional phase and the stretch reflex affects stretch-shortening cycle (Komi 2000). In vivo experiments on cats reviled that the force increase with higher speeds (Gregor, Roy et al. 1988). Even though this has been known for a long time the ability to directly apply that on the natural movement including SSC is not straightforward.

In a specific study it has been shown that up to a speed of 14·km/h the positive external work duration is greater than the negative external work duration, suggesting a contribution of muscle fibres to the length change of the muscle–tendon units. Above this speed, the two durations (<0.1·s) are similar, suggesting that the length change is almost totally due to stretch–recoil of the tendons with nearly isometrically contracting fibres (Cavagna 2006).

Triceps surae

In human triceps surae, a muscle with short fibres and a long tendon, the time courses of the total (muscle and tendon) length and of the length of the contractile component (CC) alone in running are completely different. The muscle tendon complex shows first an eccentric phase with negative work, followed by a concentric phase. The CC, on the other hand, is concentric all the time. Moreover, the work that is performed is done at a speed that guarantees a high energetic efficiency. It is argued that this high efficiency is an in-built property of the muscle mechanics for muscles with a compliant tendon and a low maximal velocity (Hof 2003).

3 Review: Modelling of the musculoskeletal system

It seems as it is an exponential increase in research performed in the area of modelling the musculoskeletal system and there are also good and recent review articles in the field (Pandy 2001; Fernandez and Pandy 2006; Viceconti, Testi et al. 2006; Erdemir, McLean et al. 2007). One of the largest areas of human movement is the human gait and also in this area a few recent review articles have been published (Zajac, Neptune et al. 2002; 2003). Because of this already good mapping of the research in modelling the musculoskeletal system the gain of knowledge has been great. A special interest has been put on the ability to better simulate movements involving high speed and large forces such as high jump, sprint running and many other sport activities. A property that increases in importance when the movement involves high speed is the stretch-shortening cycle phenomenon (Komi 2000), see 2.3 for more details.

The first valid question to ask is why there is a need of developing models of the musculoskeletal system. The alternative is to directly or in laboratory environments carry out measurements on the human body. Both these methods are needed because direct measurements are in many cases the only possible method to use but direct measurement of for example muscle forces is generally not feasible in a clinical setting, and non-invasive methods based on musculoskeletal modelling are therefore mostly considered (Erdemir, McLean et al. 2007). Dynamic simulations of movement, using a musculoskeletal model, allow one to study neuromuscular coordination, analyse athletic performance, and estimate internal loading of the musculoskeletal system. Simulations can also be used to identify the sources of pathological movement and establish a scientific basis for treatment planning (Delp, Anderson et al. 2007).

3.1 Musculoskeletal system

Phenomenological and numerical models of the musculoskeletal system are built up in many different ways depending on how the models are supposed to be used. The most accurate and sophisticated muscle models described in the literature yield infeasible computation times, even on modern supercomputers, if they are combined with optimal control techniques (Eberhard, Spägele et al. 1999). Therefore, plenty of different models are developed and a difficult part is to evaluate which model and method is best and in which cases. When using an inverse dynamic solution with static optimization a much more advanced model can be used compared to an optimal control solution but instead this optimization is only considering static conditions. A number of anatomical measurements, extremely important for biomechanical modelling, such as muscle-fibre length, tendon rest length and muscle-fibre pennation angles, can currently be obtained only via dissection (Viceconti, Testi et al. 2006). Because of this, advanced scaling tools have to be used to get the right dimensions.

There are plenty of models presented in the literature but the ability to replicate them is more or less impossible if the author of the model is not willing to supervise. As a part of the review one article was chosen to make a more thorough analysis. It turned out that 26 reference articles were needed to be able to reconstruct the model. Of these 26 references around half of them were easy to find but a few articles were considered impossible to find by the author. One of the articles was referring to unpublished material that would be sent by request which is getting quite difficult when the article is almost three decades old.

3.1.1 Complicated compared to simple model

A query that could be of great interest for a researcher is the knowledge of how complicated model that has to be used. Depending on the research question to answer different levels of complexity has to be put into the model. While simple models can be helpful in identifying basic features of muscle function, more complex models are needed to discern the functional roles of specific muscles in movement (Pandy 2003). The one of the most simple models to use is a spring-mass model which were used by Bullimore & Burn (2007) to analyse running (3-5 m/s). It showed good predictions of stance time, vertical impulse, contact length, relative stride length and relative peak force but systematically overestimated horizontal impulse, change in mechanical energy, aerial time and peak vertical displacement (Bullimore and Burn 2007). The spring-mass model is usually used to predict the external kinetic and kinematic variables of interest (Cheng and Hubbard 2004; Robilliard and Wilson 2005), or the joint torque (Cheng and Hubbard 2005).

In the study by Pandy (2003) a comparison were made between one simple and one complex model in walking. The variables of interest were how muscle forces, gravitational forces and centrifugal forces (i.e. forces arising from motion of the joints) combine to produce the pattern of force exerted on the ground. It showed that the simple model gave reasonable results for the larger questions of understanding but the far more complex model (3D) gave plenty of important detailed information (Pandy 2003).

The interest of what is going on inside the body drives the development of more complex models which includes muscles. Many models are built in two dimensions (see Table 1) making the model less complex. This introduces difficulties since the human body musculature has three-dimensional characteristics that are hard to be reduced into two dimensions. Especially, when looking at the location of the origin, insertion and via-points of most muscles, it is observed that three-dimensional vectors instead of two-dimensional vectors better represent the line of action of many muscles

(Nagano, Umberger et al. 2005). Due to that reason and the improving computer capacity many of the newer models are developed in three dimensions.

The latest in model development is to create three-dimensional (3D) finite-element models that are able to represent complex muscle geometry and the variation in moment arms across fibres within a muscle. This new framework for representing muscle will enhance the accuracy of computer models of the musculoskeletal system (Blemker and Delp 2005).

3.1.2 Bones and joints

The modelling of the bones and joints is of course dependent on the complexity of the model, but it is usually assumed that the bones are infinitely rigid and the body articulations are ideal joints (Viceconti, Testi et al. 2006). The degree of freedom in a joint is also a very important issue because the results can differ a lot. It has been shown for example that pure hinge joints are inappropriate for modelling the dynamical joint function of the knee and ankle joints. A more flexible joint representation predicted a lot of synergistic as well as antagonistic muscle activation which was also found in the EMG patterns (Glitsch and Baumann 1997).

When the physiological joint constraints are not imposed, e.g. modelling the ankle joint as a spherical joint, muscle forces can instead be overestimated. Related to kinematics, a two-dimensional musculoskeletal model will give different results than a three-dimensional model as a result of enforcing joint movements, which are naturally three-dimensional, to be in a plane (Erdemir, McLean et al. 2007). It is therefore important to use a model with the appropriate number of degrees of freedom in order to avoid overestimation of muscle forces. This means that the standard 3Djoint torques's are not necessarily a good starting point.

3.1.3 Skeletal muscles

Within the context of modelling skeletal muscles at least two types of muscle models may be important. The first is a molecular type, e.g., the sliding filament models by Huxley(1974) where the muscle actions are described at the sarcomere level by using insight into the biophysical processes. The second are phenomenological or macroscopic models, e.g. the Hill type (Winters and Woo 1990), where mathematical models and their respective parameters are derived from transfer functions between input/output data without analysis of the microscopic biomechanical/biochemical processes. Both approaches have their strengths and weaknesses. For the first approach, the correct abstraction and modelling of complex biological structures as well as the determination of model parameters seems to be difficult. The second approach often suffers from a lack of accuracy in specific situations (Eberhard, Spägele et al. 1999). The complexity of the molecular type would be far beyond what is reasonable. Therefore, some kind of phenomenological model is used in all cases of musculoskeletal modelling known by the author and usually a Hill type model (Pandy 2001).

The muscles are the only active elements which can apply forces to the skeleton. They are controllable by the central nervous system. Therefore, their accurate mathematical description is even more important than very detailed approaches for the skeleton (Eberhard, Spägele et al. 1999). Muscle's peak isometric force is usually obtained by multiplying muscle's physiological cross-sectional area (PCSA) by a generic value of specific tension (Pandy 2001). The corresponding fibre length for the maximum force and pennation angle are almost always based on data obtained from cadaver dissections (Pandy 2001).

A study performed muscle force estimates for walking and showed that the property most sensitive to changes where tendon rest length and least sensitive were muscle PCSA. These results emphasize the importance of obtaining accurate estimates of tendon rest length and muscle-fibre length, particularly for those actuators that function as prime movers during locomotion (Redl, Gfoehler et al. 2007).

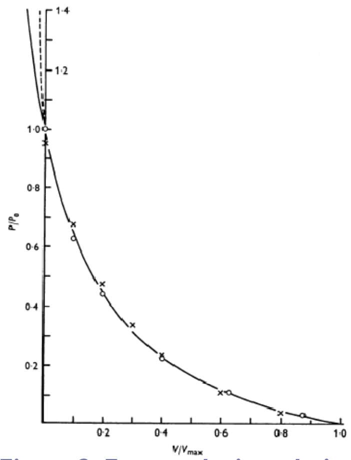

Figure 2: Force-velocity relationship (Huxley 1974)

As been stated before the Hill model is a phenomenological model. The model was first seen in literature 1939. Using the Hill model, it is possible to describe qualitatively the force-time response of the muscle (Cole, van den Bogert et al. 1996).

3.2 Algorithms for estimation of muscle forces

Model-based estimation of muscle forces usually requires optimization regardless of the strategy (inverse or forward dynamics) selected to solve for the equations describing the musculoskeletal system. The adoption of either an inverse or forward dynamics approach is typically dependent on the availability of the experimental data or the clinical/research question to be answered. (Erdemir, McLean et al. 2007)

In the literature three different methods are frequently present and these three are also described here. One of them are using inverse dynamics with static optimization, the other two are using forward dynamics one combined with assisted tracking of data and the other with optimal control formulation.

3.2.1 Inverse dynamics-based static optimizations

Muscle force estimation using gait data combined with inverse dynamics and static optimization has been practiced for almost three decades and has become a routine tool in clinical gait analysis (Erdemir, McLean et al. 2007). The muscular load sharing problem is solved for each instant in time, by minimizing an objective function (e.g. total muscle force) subject to constraints representing the equality of the sum of individual muscular moments to the joint torques calculated from the inverse dynamics analysis (Erdemir, McLean et al. 2007). Inadequate kinematic models to represent the motion of interest and inaccuracies of experimental data have been identified as weaknesses of the methodology (Erdemir, McLean et al. 2007).

3.2.2 Forward dynamics assisted tracking

Forward dynamic optimization can be performed such that solutions are less dependent on measured kinematics and ground reaction forces, and are consistent with additional knowledge, such as the force–length–velocity–activation relationships of the muscles, and with observed electromyography (EMG) signals during movement (Erdemir, McLean et al. 2007).

When muscle excitations or joint torques are available or assumed, a forward dynamics approach can be utilized that integrates the system equations to calculate the movement patterns. An initial set of muscle activations are fed into a forward dynamics model of the musculoskeletal system. The solution is compared against experimental data and the process is iterated by updating the muscle activations that best reproduce the experimental kinematics and in some cases kinetics (Erdemir, McLean et al. 2007).

The technique has been used in a variety of activities and particularly found its applications for high pace movements of sports biomechanics. A common use has been to find a set of muscle activations that can reliably reproduce the movement pattern, and subsequently perturb parameters of the optimal solution to explore injury mechanisms. This strategy is advantageous due to the more straightforward inclusion of muscle dynamics within the solution when compared to inverse dynamics-based static optimization (Erdemir, McLean et al. 2007). Although the dynamics of the muscle (activation and force generation properties) might not be influential for low pace movements, muscle force estimation for activities of high performance might benefit from this property of forward dynamics assisted data tracking (Erdemir, McLean et al. 2007).

It is possible that multiple solutions exist to track the same experimental data. Multi-objective criterion probably increased the tracking errors in favour of estimating muscular forces based on task objectives (Erdemir, McLean et al. 2007).

The approach is advantageous in that the movement is predicted. Yet, accurate knowledge of muscle excitations (forces) or joint torques is rare, eliminating the stand-alone application of this technique (Erdemir, McLean et al. 2007).

3.2.3 Optimal control strategies

Occasionally the experimental data might be incomplete or the movement related investigations require predictive simulations of the musculoskeletal system in novel situations for which no movement data are available. Under these circumstances, optimal control strategies that use forward dynamics are alternatives to solve for muscle excitations and forces during movements. Given an initial set of muscle excitations, system equations are first solved in a forward dynamics fashion. Then, the objective of the movement and task related constraints, e.g. static equilibrium at final time, are calculated. The objective can be a function of muscle force and kinematics. It can be related to task performance, e.g. maximum height jumping, and is usually represented in an integral form to introduce dependence on time history (Erdemir, McLean et al. 2007). The process is iterated until an optimal set of muscle excitation patterns is found that minimizes the objective and satisfies the constraints (Erdemir, McLean et al. 2007).

The technique allows for changes in motion and adaptations at the muscular control level following alterations in the system. This major advantage can lead to predictive simulations to assess changes in control of muscles and muscle forces as a result of therapeutic interventions, surgery and rehabilitation (Erdemir, McLean et al. 2007). However, the selection of an objective function can still be controversial; the criterion is clear for movements that aim for optimal performance (e.g. maximal height jumping) but for other activities (that rely on physiological function) such as walking at different speeds and non-ballistic movements, this selection relies on the investigators' preference (Erdemir, McLean et al. 2007). Computational complexity and implementation difficulties also prohibit the routine use of this technique in clinical settings and limit its use to research environments (Erdemir, McLean et al. 2007). Similar movement patterns can be obtained using optimal control simulations with different objective functions while investigating non-ballistic activities, but the muscle activation patterns might be different (Erdemir, McLean et al. 2007).

When using optimization techniques to predict muscle forces, it must be recognized that the solution is sensitive to many assumptions and variables such as PCSA. On the other hand, the joint force solutions are less sensitive to such variations, and the absolute values are more reliable (Brand, Pedersen et al. 1986).

3.3 Validation

All results generated from a computer model have to be validated to show that they gave reasonable results. Due to many reasons there are difficult to successfully validate the musculoskeletal computations of the muscle force estimates (Erdemir, McLean et al. 2007).

Studies of muscle force predictions usually compare muscle loading or activation patterns against EMG data as an estimate of validity. Although evaluating the temporal characteristics and intensity of muscle firing during a movement is useful, such comparisons cannot verify the magnitude of the calculated muscle force. Fortunately, alternative and more advanced analyses exist, which incorporate the quantification of muscle force sensitivity on modelling parameters and comparisons of muscle forces against direct measurements of tendon loading (Erdemir, McLean et al. 2007).

Direct validations are limited to simple musculoskeletal models, e.g. with one or two degrees of freedom, and tendon force measurements are performed on animals by surgical implantation of tendon force measurement devices. Nonetheless, the results of these studies can be used to assess the validity of objective functions used in inverse dynamics-based static optimization and the load sharing between synergistic muscles (Erdemir, McLean et al. 2007).

It is possible to predict similar muscle forces and joint reaction forces for walking using the inverse dynamics-based static optimization approach and the optimal control simulation approach. The consistency observed in these muscle force predictions suggests that if experimental accuracy can be improved, then resultant muscle forces might not depend on the simulation characteristics (Erdemir, McLean et al. 2007).

Induced acceleration analysis (IAA) provides a platform to establish the link between an isolated change in a muscle force and the corresponding changes in the movement. This “coupled dynamics” representation can explain some of the counterintuitive functions of biarticular muscles, such as the gastrocnemius functioning as knee extensor for specific conditions (Erdemir, McLean et al. 2007).

3.4 Musculoskeletal models in literature

The number of musculoskeletal models in literature is very large due to the large amount of different implementations. First of all there are a very simple models only using simple spring-mass models (Bullimore and Burn 2007) to very advanced models with plenty of DoF and muscle groups included (Anderson and Pandy 1999). Depending on the choice of algorithms for estimating muscle forces (3.2) different complexity of the model is allowed where inverse dynamics methods can have very complex models compared to optimal control strategies.

A special interest within this thesis was explosive movements including high speed and large forces. Consequently, the inverse dynamics that uses a static optimization is not considered as an alternative due to poor results in faster movements. A forward dynamic configuration is more appropriated to use. Further, often the aim is to find optimal movement patterns and therefore no available measured data exist to use a tracking configuration. The commonly used method is therefore an optimal control strategy. The models presented below are, by the reasons described above, models used in optimal control strategies for estimating muscle forces in movements with high speed and large forces (vertical jumps).

3.4.1 Studies investigating vertical jumps (optimal control strategy)

In a study conducted 1993 (Anderson and Pandy 1993) subjects jumped on average 5% higher during the counter-movement jump (CMJ) than they did during the squat jump (SJ), although some subjects performed equally well during both jumps. The model, on the other hand, jumped 2% higher during the SJ than it did during the CMJ. In that study the total energy delivered to the skeleton was almost the same for the CMJ and the SJ. It was also noticed that there was almost as much elastic strain energy stored during the SJ as it was stored during the CMJ. Calculations indicate that much more energy was lost as heat during the CMJ than the SJ. With this analytical result in mind, together with their own analytical and experimental findings, the authors propose that humans perform countermovements not so much to store and re-utilize elastic strain energy during jumping, but rather to increase ground contact time during the propulsion phase of the jump.

Several years later, the same researchers made new more advanced model and analyse (Anderson and Pandy 1999). The mode1 was characterized by several key features: first, it was a mode1 of the whole body; second, full three-dimensional motion was permitted by virtue of a 6 dof pelvis, 3 dof joints for the back and the hips, and 2 dof joints for the ankles; third, the feet were free to make and break contact with the ground; and fourth, the number of muscles was much greater than that considered in previous dynamic optimization studies. This increase in complexity has improved the fidelity of the mode1 in a number of ways: (1) the vertical ground-reaction force demonstrated a more gradual decrease near lift-off compared with the results obtained in previous simulations (Pandy and Zajac 1991); (2) the fore-aft ground-reaction force was reproduced more accurately than before (Pandy and Zajac 1991); and (3) the mode1 was capable of predicting not only the major movements of the body segments in the sagittal plane, but also those which occur in the frontal and transverse planes. The major limitation of the mode1 was its failure to reproduce the kinematics of the jump near lift-off. This result may be explained by the relatively fast rise time for muscle activation used in the model. Overall, however, the high leve1 of agreement between mode1 and experiment validates many of the parameters assumed in the model. Since the interaction between the feet and the ground was modelled efficiently, the model is well suited to simulating three-dimensional gait (Anderson and Pandy 2001).

Table 1: Previous studies simulating vertical jumps. Dim = dimension , Seg = segments, DoF = degrees of freedom

Type of computation	Activity	Objective	Dim	Seg	DoF	Driven	Controls	Year	Reference
Optimal control	Vertical jump	Maximum height	3D	9	20	32 MG		2007	Nagano et al. (2007)
Optimal control	Vertical jump	Maximum height	3D	9	20	32 MG	Modelled as a series of step functions with constant duration	2005	Nagano et al. (2005)
Optimal control	Vertical jump	Maximum height	2D	4	4	6 MG	Defined by time onset of maximal activation	2001	Bobbert (2001)
Optimal control	Vertical jump	Maximum height	3D	10	23	54 MG	Linear interpolation	1999	Anderson and Pandy (1999)
Forward dynamics assisted data tracking	Vertical jump		2D	4	3	9 MG	Approximated by polynomials	1999	Spägele et al. (1999)
Optimal control	Vertical jump	Maximum height	2D	4	4	8 MG	Linear interpolation	1992	Pandy et al. (1992)
Optimal control	Vertical jump	Maximum height	2D	4	4	8 MG	Bang-bang	1991	Pandy et al. (1991)
Optimal control	Vertical jump	Maximum height	2D	4	4	8 MG	Bang-bang	1990	Pandy et al. (1990)

The study conducted by Bobbert (2001) had the aim to determine the dependence of human squat jump performance on the compliance of series elastic elements (SEEs) of the triceps surae and to explain this dependence. The three-dimensional musculoskeletal model by Nagano, Komura et al. (2005) was developed using DADS-3D (LMS CADSI, Coralville, IA, USA) with the FORTRAN- based USER.FORCE option. The neuromuscular model has nine rigid body segments, 20 degrees of freedom, 32 Hill-type lower limb muscles actuators.

3.5 Available software

It has been an increase in research in the area of modelling the musculoskeletal system. The continuously improving computers and the fact that it is very time consuming to build own models have driven the development of commercial and open source programs. Presented below are some of the largest and most used software's

SIMM

Delp & Loan (1995) have created a graphics-based software system that enables users to develop and analyse musculoskeletal models without programming. The origin of the program can be found in the doctoral thesis by Delp (1990) To define a model using this system one specifies the surfaces of the bones, the kinematics of the joints and the lines of action and force generating parameters of the muscles. Once a model is defined, the function of each muscle can be analysed by computing its length, moment arms, force and joint moments. The software has been implemented on a computer graphics workstation so that users can view the model from any perspective and graphically manipulate the joint kinematics and musculoskeletal geometry. Models can also be animated to visualize the results of motion analysis experiments (Delp and Loan 1995).

AnyBody

Recently, the Danish research team Damsgaard, Rasmussen et al. (2006) released the commercial software *AnyBody Modelling System* which is capable of analysing the musculoskeletal system of humans or other creatures as rigid-body systems. The software includes features as the inverse dynamic analysis that resolves the fundamental indeterminacy of the muscle configuration. In addition to the musculoskeletal system, a model can comprise external objects, loads, and motion specifications, thereby providing a complete set of the boundary conditions for a given task (Damsgaard, Rasmussen et al. 2006).

Musculoskeletal Modelling in Simulink and Virtual Muscle

Simulink models of the musculoskeletal system can be created using two software packages, Musculoskeletal Modelling in Simulink (MMS) and Virtual Muscle (VM). In addition, there is a need of the commercial software package SIMM (Musculographics Inc., USA) for importing models. MMS converts anatomically accurate musculoskeletal models generated by SIMM into Simulink© blocks. It also removes run-time constraints on kinetic simulations in SIMM, and allows the development of complex musculoskeletal models without writing a line of code (Davoodi, Brown et al. 2003).

Virtual Muscle builds realistic Simulink models of muscles responding to either natural recruitment or functional electrical stimulation (FES). Models of sensorimotor control systems can be developed using various Matlab© (Mathworks Inc., USA) toolboxes and integrated easily with these musculoskeletal blocks in the graphical environment of Simulink (Davoodi, Brown et al. 2003).

OpenSim

OpenSim is a freely available open-source software system that lets users develop models of musculoskeletal structures and create dynamic simulations of a wide variety of movements. Delp et al. (2007) are using this system to simulate the dynamics of individuals with pathological gait and to explore the biomechanical effects of treatments. OpenSim provides a platform on which the biomechanics community can build a library of simulations that can be exchanged, tested, analysed, and improved through a multi-institutional collaboration. (Delp, Anderson et al. 2007).

4 The musculotendon-unit model

As been stated earlier, the development of a new musculoskeletal model is not trivial and therefore not realistic to fit into a master thesis. The work of this thesis was concentred on the development of a musculotendon (MT) -unit model. As the name describe this unit consists of the muscle and its belonging tendon structure. An important criterion for the model was to make it dimensionless so the same model could be used to describe different muscles in the body even though they have different properties and dimensions. The scaling parameters used were the maximum isometric muscle force ($F_{ISO,Max}$) and the muscle length corresponding to the maximum isometric force ($l_{M,opt}$). During the meticulous review of literature many different MT-unit models were found as can be reed earlier (3.1.3). A decision was made to use the model reported by Pandy, Zajac et al. (1990). Even though this article is almost two decades old, the model is still used and the subject of the article were vertical jumping which includes both high speed and large forces. The MT-unit model in the chosen article was first presented at the RESNA conference 1986 (Zajac, Topp et al. 1986) and has been cited many times after.

Another question for discussion was the type of programming environment that should be used. The literature are showing a wide spread of environments. Finally decisions were made to develop the MT-unit model in *Mathematica* (Wolfram Research Inc. 2007). The decision was made mostly due to earlier familiarity with the program and its ability to treat both symbolic and numerical mathematics.

When talking about the original article or original graph it refers to Zajac et al. (1986).

4.1 MT-unit

The MT-unit is based as been said on Zajac et al. (1986) which was using a Hill-type model. The model consists of a tendon and a muscle (Figure 3). These two components will be described in detail later.

The idea of the model was to build it up using springs and actuators. The representation is basically done in a schematic way of the representation of a real human musculotendon unit. The tendon model (T) is placed in series with the muscle model (M) and represents by a spring. The muscle model consists of a parallel elastic element (PE), a serial elastic element (SE) and a contractile element (CE) (see Figure 3). Both the elastic elements are represented by simple springs and CE is represented as an actuator.

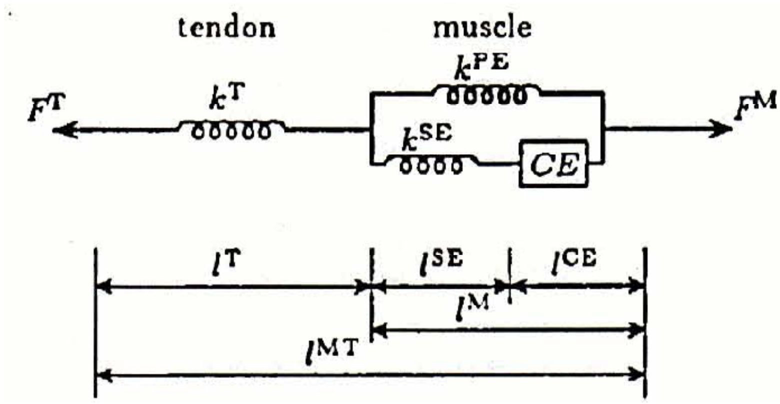

Figure 3: The musculotendon-unit. The stiffness symbol k^i is not used in this report but it stands for the tangent stiffness. Reproduced from Zajac et al. (1986)

In this chapter many symbols are used and many of them are explained below:

$F_i -\ force\ in\ ith\ element$
$\lambda_i -\ normalised\ length\ in\ ith\ element$
$l_i -\ lenght\ of\ ith\ element$
$l_{M,opt} -\ length\ of\ muscle\ at\ F_{ISO,Max}$
$\mu_i -\ normalised\ velocity\ of\ ith\ element$
$v_i -\ velocity\ of\ ith\ element$
$\phi_i -\ normalised\ force\ in\ ith\ element$
$F_{ISO,Max} -\ maximal\ isometric\ force$
$\alpha - normalised\ muscle\ activation$
$i = MT, M, T, PE, SE, CE$

All lengths were made dimensionless by the muscle length at maximal isometric contraction ($\lambda_{M,opt}$) and the forces by the maximum isometric force ($F_{ISO,Max}$).

4.1.1 Muscle

The components of the muscle are as earlier stated the parallel elastic element (PE), the serial elastic element (SE) and the contractile element (CE). The individual properties of the components are described separately in own sections below.

The length of PE (λ_{PE}) is the same as for M and the length of SE and CE together gives the length of M and that is represented in equations below.

$$\lambda_{PE} = \lambda_M \qquad \text{(Eq. 1)}$$
$$\lambda_M = \lambda_{SE} + \lambda_{CE} \qquad \text{(Eq. 2)}$$

The force of M is the sum of the force in SE and PE and the force in CE is equal to the one in SE and that is shown below.

$$\phi_{CE} = \phi_{SE} \qquad \text{(Eq. 3)}$$
$$\phi_M = \phi_{SE} + \phi_{PE} \qquad \text{(Eq. 4)}$$

This gives that at maximal isometric contraction the length of M is exactly one because they are made dimensionless.

Parallel elastic element

The purpose of the parallel elastic element was to simulate the force arising from either inter-fibre connections or elastic structures internal to the muscle fibre (Zajac, Topp et al. 1986). This was simulated by a simple spring and the force was assumed to be zero when the muscle was shorter than the optimal length. Further, it was assumed that this relationship was the same among all the muscles (Zajac, Topp et al. 1986).

$$F_{PE} = k_{PE}\, l_{PE} \qquad \text{(Eq. 5)}$$

The constitutive equation of the passive muscle was viscoelastic, as it was for most soft tissues. For slow movements, the viscous contribution was neglected and hyperelastic models were used for the constitutive equation. For more rapid movements, the combination of viscous forces and large deformations makes the models extremely nonlinear, and it was necessary to adopt explicit integration schemes to solve them (Viceconti, Testi et al. 2006). In this case the equation for PE was derived using a graph in the original article. The force equation (Eq. 6) were constructed by localization of the points (1.0, 0.0), (1.3, 1.0), (1.2, 0.5) from the original graph (Figure 5) and then make a curve fit for a second order polynomial.

$$\phi_{PE} = 7.5 - 15.8\,\lambda_{PE} + 8.3\,\lambda_{PE}^2 \quad when \quad \lambda_{PE} > 1 \qquad \text{(Eq. 6)}$$

$$\phi_{PE} = 0 \quad when \quad \lambda_{PE} < 1$$

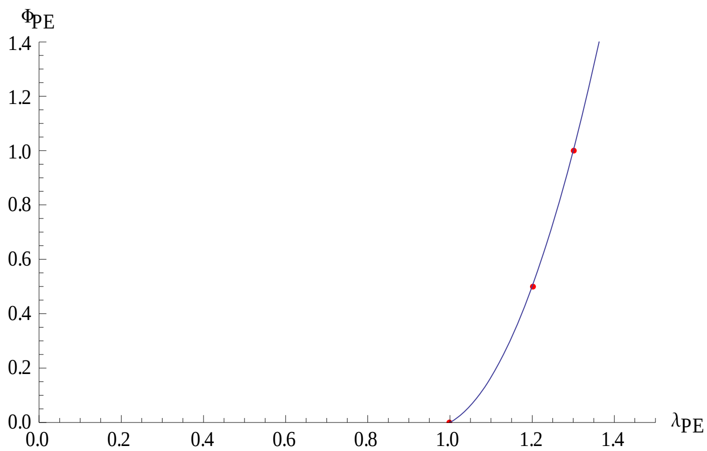

Figure 4: Force-length relationship of PE (Eq. 6).

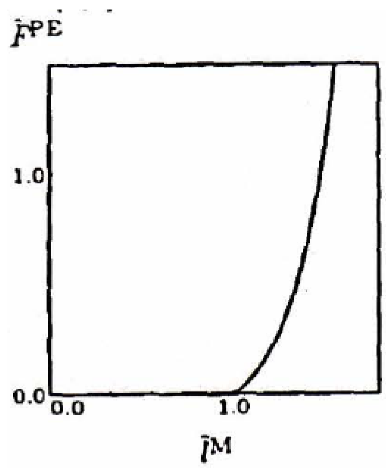

Figure 5: Force-length relationship of PE. The symbols used in this graph is the representing the same thing as in the graph to the left. Reproduced from Zajac et al. (1986)

Serial elastic element

The stiffness of an active muscle is simulated by the serial elastic element (SE). This elasticity is due to the elastic components of the cross-bridges (Huxley 1974).

$$\phi_{SE} = k_{SE}\, l_{SE} \qquad \text{(Eq. 7)}$$

By studying the original graph (Figure 7) the following differential equation can be put up:

$$\phi'_{SE}(l) = 10 + 100\, \phi'_{SE}(l_{SE}) \qquad \text{(Eq. 8)}$$

This equation can be solved and the constant Q_1 can be solved by putting the length to the one at maximal isometric contraction ($\lambda_{SE,ISO}$=0.284546) and the force at maximal isometric contraction ($F_{SE,ISO}$=1). The equation and constant are shown below.

$$\phi_{SE} = \phi_{SE}(\lambda_{SE}) = -\frac{1}{10} + Q_1 e^{100\,\lambda_{SE}} \qquad \text{(Eq. 9)}$$

$$where\ Q_1 = 4.83 \times 10^{-13} \quad and \quad \lambda_{SE,ISO} = 0.284546$$

To calculate the exact tendon slack length of SE the force was set to zero and λ_{SE} was solved giving the following result:

$$\lambda_{SE0} = 0.260567 \qquad \text{(Eq. 10)}$$

Due to the fact that SE only manage tensile stretches it was not be able to generate any force when the length of SE was shorter than the slack length ($\lambda_{SE}<\lambda_{SE0}$). Because of the numeric's, the force in SE are never put to zero, a very small number (10^{-3}) is used during these conditions.

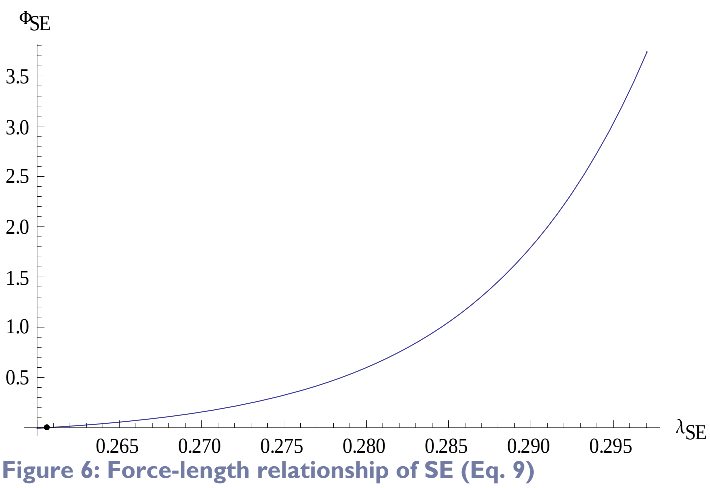

Figure 6: Force-length relationship of SE (Eq. 9)

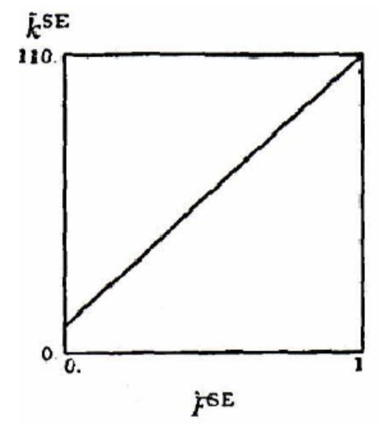

Figure 7: Stiffness-force graph of SE. Reproduced from Zajac et al. (1986)

Contractile element

The contractile element is the only active element in the MT-unit. The force of the contractile element depends of its length, velocity and activation (Zajac, Topp et al. 1986; Erdemir, McLean et al. 2007).

$$\phi_{CE} = \phi_{CEL} \cdot \phi_{CEV} \cdot \alpha \qquad \text{(Eq. 11)}$$

$$\textit{where } \phi_{CEL} \textit{is the normalized force in CE depending on the length and } \phi_{CEV} \textit{ depending on the velocity}$$

Force-length dependence

The force-length dependency is based on the amount of overlap of the myofilaments under the assumption of sarcomere and muscle fibre homogeneity. The same force-length curve could be used for all muscles (Zajac, Topp et al. 1986).

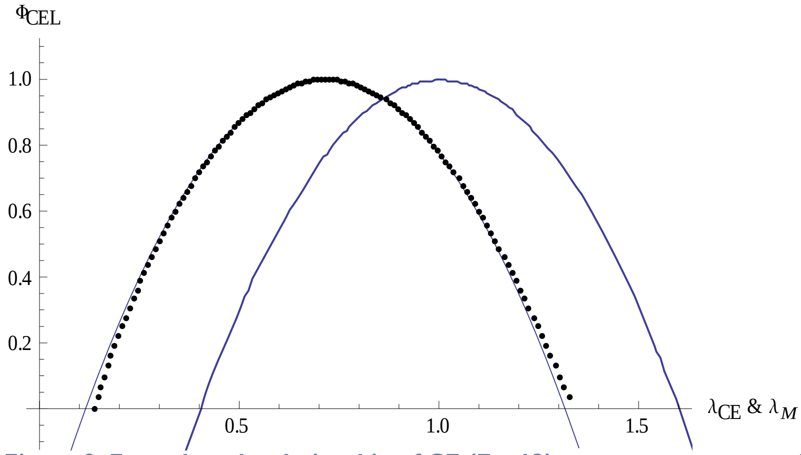

Figure 8: Force-length relationship of CE (Eq. 13)

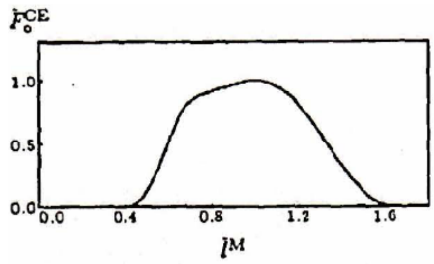

Figure 9: Force-length relationship from original article. Reproduced from Zajac et al. (1986)

To derive the force-length relation was the greatest challenge compared to the other parts of the MT-unit. The original article was only presenting a graph were the force depends of the total muscle length (Eq. 2) and not on the length of the contractile element which should be the case. One reason for this presentation could be that it is uncommon to include a serial elastic element (SE) in Hill-type muscle models. For that reason, the graph from the original article has to be transformed to depend on λ_{CE} instead of λ_M.

From the existing graph (Figure 9) following points were used; (0.4, 0.0), (1.0, 1.0) and (1.6, 0.0). These points were used to fit a sinusoidal function by the *Matematica* function *Fit:*

$$\phi_{CEL}(\lambda_M) = \max\left[-1.27 - 3.46\,\lambda_M + 6.08\,\sin\lambda_M\ , 0\right] \qquad \text{(Eq. 12)}$$

where max gives the algebraically largest of its arguments.

This equation for the length dependence was then used together with the force equation for SE (Eq. 9). The force in SE and CE should always be the same and this is used in the transformation of F_{CEL} to depend on CE instead of M. If the velocity is zero and the activation is constant maximum (=1) the only variable is the length dependence (Eq. 11). The dependence is calculated using a for-loop were

λ_M is increased from 0.4 to 1.6 with a length step of 0.02. Within the for-loop the force for $\phi_{CEL}(\lambda_m)$ were calculated and that gave F_{SE} and then the length λ_{SE} can be calculated (Eq. 9). The final step was to subtract λ_{SE} from λ_M to get λ_{CE} (Eq. 1) and by that get the force-length dependence to depend on λ_{CE}.

$$\phi_{CEL}(\lambda_{CE}) = \max\left[-0.419 - 3.97\,\lambda_{CE} - 2.77\,\lambda_{CE}^2\,, 10^{-3}\right] \qquad \text{(Eq. 13)}$$

where max gives the algebraically largest of its arguments.

This equation is plotted in Figure 8. Because of the numeric's the force (ϕ_{CEL}) is never put to zero instead a very small number (10^{-3}) is used during these conditions.

Force-velocity dependence

Due to the cross-bridge dynamics the contractile element depends on the velocity of shortening and lengthening and with temperature (Huxley 1974).

Figure 11 shows the graph of the force-velocity relationship from the original article. Due to convenience reason this graph was rotated anticlockwise 90 degrees before it was replicated. The chosen points were; (-1.0, 0.0), (0.0, 1.0), (2.0, 1.4) and (-0.2, 0.5). The force-velocity curve has similar shape as an arc tan-function and therefore this kind of function were chosen to fit against the points. That gave the equation:

$$\phi_{CEV} = \phi_{CEV}(\lambda_{CE}) = a + \frac{atan(b + c\,v_{CE})}{d} \qquad \text{(Eq. 14)}$$

$$a = 0.672 \quad b = 0.796 \quad c = 5.808 \quad d = 2.046$$

This equation is plotted in Figure 10.

According to the original article the fastest contraction possible for the muscle is $\mu = -1$ and the fastest elongation of the muscle is $\mu_{CE} = 2$.

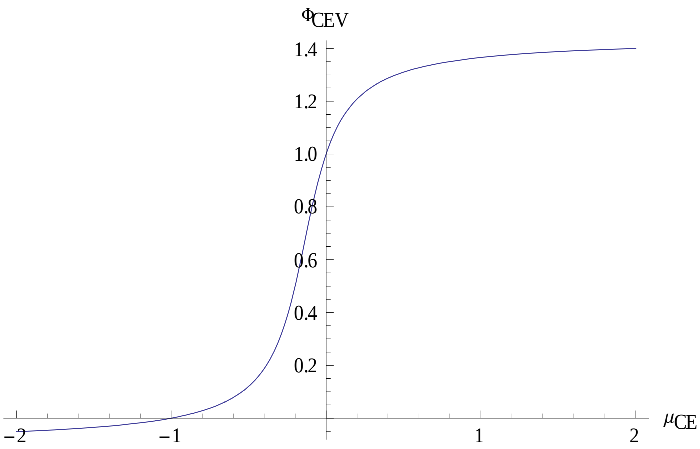

Figure 10: Force-velocity relationship of CE (Eq. 14)

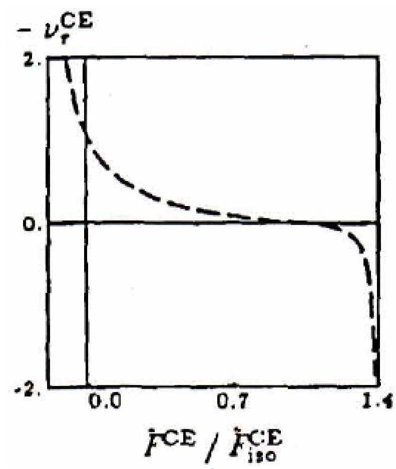

Figure 11: Force-velocity graph. Reproduced from Zajac et al. (1986)

The maximum shortening velocity (v_{max}) of the muscles can be adjusted to their optimum values for the tasks required of them(Alexander 1991). When the muscles are stretched and do negative work, the force rises and the rate of ATP splitting falls, so economy increases (Alexander 1991).

Activation

The activation is only an amplifier which means that the amount of force produced increase but it is not changing the force-length or force-velocity curves. The activation is put to a constant value before simulation which means that the muscle cannot change its level of activation during the simulation. The case of constant activation in a muscle has a very narrow field of applications. Suggested case where this could be a good approximation is calf muscles during ground contact of a maximal vertical drop jump.

The reason for having a constant activation is to reduce the complexity of the model but the implementation of the activation should be developed further if the model is considered to be used in more complex contexts.

4.1.2 Tendon

The tendon element (T) of the model represents the physiological tendon both internal and external to the muscle. The strain in the tendon is assumed to be the same everywhere in the tendon. Further, it is assumed that the force-strain relationship is the same among all musculotendon units. The tendon slack length is varying a lot depending of the muscle (Pandy, Zajac et al. 1990) and is therefore change for the specific musculotendon unit.

$$\epsilon_T = \frac{\lambda_T - \lambda_{T0}}{\lambda_{T0}} \qquad \text{(Eq. 15)}$$

The original article presented a graph (Figure 13) over the relationship between force and strain and within this graph three points were located; (0.0, 0.0), (0.03, 1.0) and (0.02, 0.5). A second order polynomial was used as fitting function and gave the following function:

$$\phi_T = \frac{25}{3}\,\epsilon_T + \frac{2500}{3}\epsilon_T^2 \;\; when \;\; \epsilon_T > 0 \qquad \text{(Eq. 16)}$$

$$\phi_T = 10^{-5} \;\; when\, \epsilon_T < 0$$

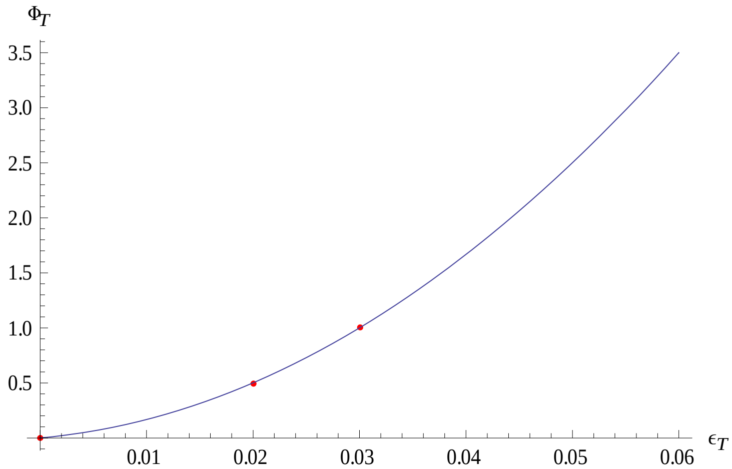

Figure 12: Force-strain relationship of T (Eq. 16).

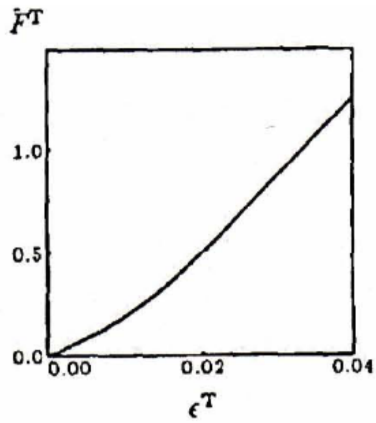

Figure 13: Force-strain graph of T. Reproduced from Zajac et al. (1986)

Tendons are usually represented as an elastic element. Even though force varies nonlinearly with a change in length as tendon is stretched from its rest length, a linear force-length curve is sometimes used. This simplification will overestimate the amount of strain energy stored in tendon (Pandy 2001).

4.2 Numerical calculations

Last part described the components one by one but they have to be put up to a system representing the musculotendon unit. Due to the complexity of the system two configurations of numerical calculations were used; starting configuration and dynamic configuration. As the name reveals the starting configuration was used before the simulation to find a stable starting equilibrium for the MT-unit. The equilibrium values from the starting configuration were then used as starting values in the dynamic configuration. These two steps had to be conducted because the dynamic configuration needed exact starting values and were not able to generate them itself.

The section of numerical calculations is divided into two parts; starting configuration and dynamic configuration.

4.2.1 Starting configuration

The basic thought of the starting configuration was to run a simulation in time where no input values were change and a final stable equilibrium was found.

This configuration was developed only because of the complexity of the numerics and therefore many input values did not needed a physiological explanation. Because the aim was to find a stable equilibrium, the velocity of CE was set to zero ($\mu_{CE}=0$). The simulation time was set to 4.5 seconds with a relatively large time step (=0.1) and was chosen because it gave good values for all tried cases. The only input value that was changing dependent on the simulation performed was the length of the MT-unit (λ_{MT}). This length was of course changing depending of the starting position.

To be able to solve for the whole MT-unit the use of a parameter solving algorithm needed to be used. This was because the system is highly nonlinear and includes many if-statements. At each time step a special algorithm was needed to solve equilibrium between the forces $\phi_M = \phi_T$ and $\phi_{CE} = \phi_{SE}$. The algorithm was based on a while statement.

The length of the tendon was used in the while statement, with an old (λ_{TG}) and a present (λ_T) value of the tendon length. These two were compared in the while statement and when the difference between them was less than the tolerance limit ($\alpha s=10^{-12}$) the solution were satisfying.

Inside the while statement the mean of λ_{TG} and λ_T were calculated and became the new λ_T. As a result of changing λ_T the lengths that depend on it had to be updated (λ_M, λ_{PE}, λ_{SE}).

The problem was that the length of SE depends on the force which by itself depends on the force of CE. Consequently, the same procedure that was explained above for the tendon was used here too but for λ_{SE}. After the new λ_{SE} was calculated the length of CE was updated.

The velocity of CE was thereafter calculated by subtracting the present λ_{CE} with the one from last time step, this was then divided by the time step length. This formula is used for all time steps except the first when the velocity was considered zero. The force of CE can then be calculated and because the force of SE should be the same this force was used in the force equation for SE (Eq. 9) and the new λ_{SE} was solved. This was looped until it satisfied the tolerance.

Thus, all the lengths were updated and consequently the force of M could be updated. Because the force of M should equal the force in T the force in M was used to solve λ_T using the equation for calculating the tendon force (Eq. 16). This was looped until it satisfied the tolerance.

The last thing done at every time step was to update λ_{CE} for use to calculate the velocity in CE at the next time step.

4.2.2 Dynamic configuration

A starting value of the length of CE has to be known to be able to run the dynamic configuration. This value was the most important outcome from the starting configuration. As the starting configuration was in a static equilibrium the velocity of CE was set to zero. The time step was set to a constant with the length 10^{-4} s.

The input value was the length of the MT-unit which could come from a simple function or from a larger musculoskeletal system simulation. The driving variable in the simulation was the length of CE which was updated without any ability for correction and was updated according to this equation:

$$\lambda_{CE}^{n} = \lambda_{CE}^{n-1} + v_{CE}\, dt \qquad \text{(Eq. 17)}$$

This equation was valid for all cases except if the minimum value of λ_{CE} were reached. In that case the length was kept constant at the minimum length.

A while statement was used to solve the length distribution between T and SE. It had the same basic thoughts as in the starting configuration algorithm. Here the while statement was driven by an old and a new λ_{SE}. The mean was taken of these two and generated the new λ_{SE} which was used to calculate λ_M and update λ_T and λ_{PE}. Having all the lengths, the force in SE was calculated using the force equations of T (Eq. 16) and PE (Eq. 6). Using the force equation for SE (Eq. 9), the length of SE was solved. When the tolerance ($\alpha=10^{-10}$) was reached the loop stopped.

The final thing in the end at every time step was to calculate the velocity of CE which was used to update the length of CE in the next step. The force generated due to the velocity was calculated according to:

$$\phi_{CEV} = \frac{\phi_{SE}}{\phi_{CEL}\, \alpha} \qquad \text{(Eq. 18)}$$

The velocity of CE could then be calculated by using the force-velocity equation (Eq. 14). If this equation would generate a value larger than 2 or less than -1 the values were corrected to these extreme values. In the situation with values larger than 2 this was noticed because this was a case of rupture of the muscle.

5 Simulation

The model developed in the last chapter is of no or very little use alone. The purpose of the MT-unit model is that it should be incorporated in a musculoskeletal (MS) model. The MS model could include up to 54 muscle groups (MG) (Anderson and Pandy 1999), each represented by one MT-unit and their specific muscle properties. It is when these kinds of MS models are included in simulations that a good MT-unit is of great use.

The choice of simulation was greatly dependent of the amount of working hours that reasonably could be placed on the simulation. The time consumption for building up and running a complex simulation with a complex musculoskeletal model is way too large to fit in the limits of this master thesis. Therefore, the simulation is performed using a musculoskeletal model consisting of only one degree of freedom, two segments and one muscle (*m. soleus*).

This chapter will describe the developed MS model including the MT-unit, make a description of the performed simulation and present the results from the simulation.

5.1 Musculoskeletal model

As been stated above the musculoskeletal (MS) model was aimed to be very simple and was therefore introducing many assumptions. The first assumption was that the model was developed in two dimensions (2D) instead of the three dimensions (3D) a real human have. The movement in the transversal plane were assumed to be small and neglected. Further, only two segments were included in the model; the foot and the shank. In Figure 14 the two segments can be seen, where the shank starts at the knee and ends at the ankle and the foot segment starts at the ankle and ends at ground contact. The other two thicker lines in the foot are just for visual clarity. The thinner line starting from the shank and attaching to the foot is representing the only muscle included in the model, *m. soleus*.

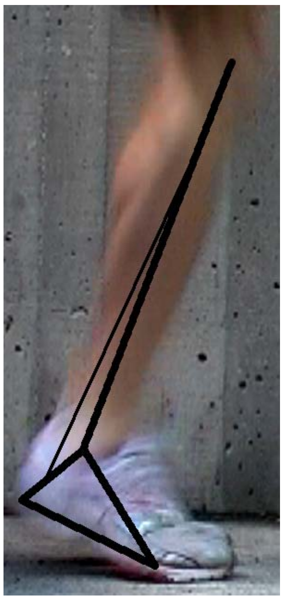

Figure 14: The MS model

The MT-unit model requires three muscle specific parameters; maximal isometric force, optimal fibre length at maximal isometric force and the tendon slack length (see Table 2). Table 2 shows values from three different sources with quite different values. One reason could be that different sizes of humans have been used and another that the pennation angles are different. The one used in this model is the values from OpenSim.

Table 2: Muscle specific parameters of m. soleus.

Muscle specific parameters	OpenSim	Article 1	Article 2
Maximal isometric force	4000N	3150N	4235
Optimal fibre length	0.08m	0.030m	0.034
Tendon slack length	0.22m	0.264m	0.360
% - tendon	73.3%	89.8%	91.4

OpenSim – generic values of a model, Article 1- (Thelen 2003), Article 2 - (Pandy, Zajac et al. 1990)

The segments were numbered so that the foot was given one and the shank two. These numbers were used for their mass (m_i), length to centre of gravity (l_{ci}), length (l_i) and inertia (I_i), see Table 3. Also two absolute angles were introduced according to Figure 15, θ_1 and θ_2. These angles were very convenient when performing calculations but not according to anatomical functions such as MT-unit moment arms. Therefore, two more angles represented in degrees were introduced and calculated as followed:

$$\theta_{foot} = \frac{180\,\theta_1}{\pi} - 34 \quad \text{(Eq. 19)}$$

$$\theta_{ankle} = \frac{180\,\theta_1}{\pi} - 34 + 90 - \frac{180\,\theta_2}{\pi} \quad \text{(Eq. 20)}$$

The foot angle, θ_{foot} , is the angle between the ground and the sole of the foot. The ankle angle, θ_{ankle} , is the angle between the shank and sole of the foot and gives zero when they are perpendicular. When the angle is less than 90 degrees it gives negative values and lager than 90 degrees positive values.

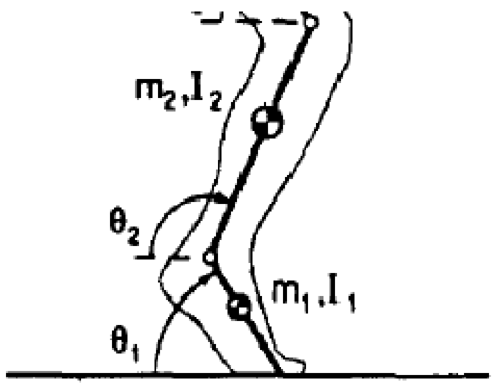

Figure 15: The MS-model. Reproduced from Pandy el al., (1990)

The human of which all anthropometric data was based on had the total mass of 76 kg. When studying Table 3 four segments are recognized but in this model only the shank and foot were modelled. The thigh and HAT were only integrated by placing a point mass in the knee so the length and inertia for those were not implemented in this model.

Table 3: Anthropometric data of the human used in this simulation (Pandy, Zajac et al. 1990). HAT stands for Head, Arms and Trunk. The mass for the leg parts is both legs added together.

	Mass (kg)	Length to COG (m)	Length (m)	Inertia (m^4)
Foot	2.2	0.095	0.175	0.008
Shank	7.5	0.274	0.435	0.065
Thigh	15.15	0.251	0.400	0.126
HAT	51.22	0.343	0.343	6.814

In the beginning of this chapter it was stated that the model only have one degree of freedom (DoF) but right now two DoF have been introduced, θ_1 and θ_2. The model was made simpler by introduce a constraint at the knee, where the horizontal movement were restrained and put to zero (equal to the ground-foot contact). This made it possible to express θ_2 in θ_1 as shown below:

$$\theta_2 = acos(-\frac{l_1}{l_2}\cos\theta_1) \qquad \text{(Eq. 21)}$$

All the parameters needed for the MS model have now been introduced so the next step was to solve the system and derive the equation of motion which was done using Lagrange's method. The generalized coordinate chosen was θ_1 and used in Lagrange function:

$$L = T(q,\dot{q}) - V(q) \qquad \text{(Eq. 22)}$$

where L is the Lagrangian, T the kinetic energy, V the potential energy and q the generalized coordinate.

5.1.1 MT-unit moment arm

One important factor in a good MS-model is to give the MT-units appropriate moment arms. The moment arm is changing depending on joint angle, muscle contraction and muscle paths. In the present model only the dependence of the joint angle was treated which has the largest influence. The angle-moment arm relationship was taken from SIMM (MusculoGraphics Inc. 2004) from a generic model. This raises a source of error due to the fact that the moment arm depends on the size of the human. SIMM generated a table of points which then were fitted to a second order polynomial using Mathematica 6.

$$r_{MT} = 0.0414 - 2.37\times10^{-4}\,\theta_{ankle} - 5.55\times10^{-6}\,\theta_{ankle}^2 \qquad \text{(Eq. 23)}$$

where θ_{ankle} is represented in degrees.

5.1.2 Length change of MT-unit

A part of the modelling of MS was to give the MT-units, in this case only one, a realistic length and length change. This means that appropriated origins and insertions should be chosen. Further, many muscles does not have a straight muscle path between these two points which influence the length and length change.

In this model only *m. soleus* was modelled and that is a simple muscle in the sentence of origin, insertion and muscle path. The length depends mainly on the angles of the joints and in this case the angle of the ankle (θ_{ankle}).

$$l_{MT} = \sqrt{\begin{array}{c}\left(l_1 \cos(\theta_1) + 0.7\, l_2 \cos(\pi - \theta_2) - 1.1\, l_1 \cos\left(\theta_1 - \frac{2\,\pi}{18}\right)\right)^2 + \\ \left(l_1 \sin \theta_1 + l_2 \sin(\pi - \theta_2) + 1.1\, l_1 \sin\left(\theta_1 - \frac{2\,\pi}{18}\right)\right)^2\end{array}} \qquad \text{(Eq. 24)}$$

This equation was applied so reasonable values for length and length change were obtained.

5.2 Drop jump simulation

The simulation itself is aiming to replicate the contact phase during a drop jump. This is a fast movement with large forces which is included in many sports (Stålbom, Holm et al. 2007). The muscle was assumed to be fully activated during the whole ground contact which was believed to be reasonable.

The maximum isometric force for *m. soleus* was set to 7000N instead of the earlier stated 4000N, for the reason that more plantar flexor muscles are usually active during this kind of activity and because *m. soleus* was the only implemented muscle in this simulation more force was given to it.

The starting angular velocity of the foot (θ_{foot}) and ankle angle (θ_{ankle}) were -353 °/s and 471 °/s, respectively. This corresponds to a drop jump from 50 cm. The reason of presenting it in degrees is due to convenience of comparing it to the literature.

5.2.1 MS-model

The MS-model was developed to be simple and it had the major aim to serve as a tool for evaluating the developed MT-unit. Even though the model was supposed to be simple it still needed to serve as a sufficient base for evaluating the MT-unit. The result from the MS-model had two important roles; describing the conducted simulation and give a brief idea of the ability of generate accurate values for the evaluation of the MT-unit.

The contact time during this analysis was 0.22 s. Figure 16 shows the two angles used to describe the position of the shank and foot in degrees. The upper curve is representing the foot angle and the lower the ankle angle. As can be seen the downward movement was going faster than the following upward movement. The largest moment arm for the MT-unit was shortly before the lowest part in the jump (Figure 17).

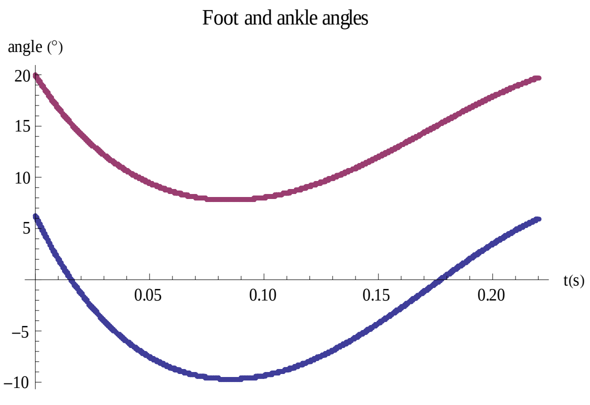

Figure 16: The angles of the foot

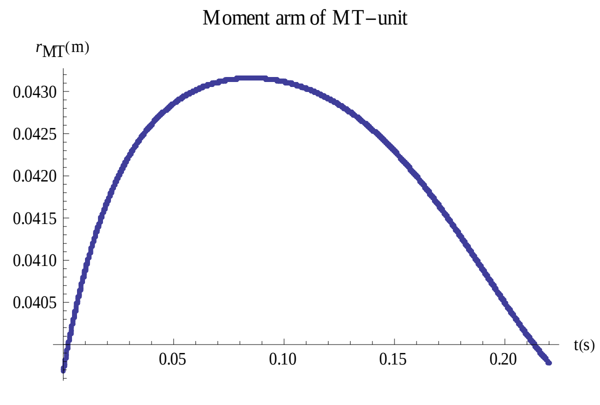

Figure 17: The MT-unit moment arm

Figure 18 is showing five pictures, from left to right, were the first shows the start position and the last the end position. The range of motion was approximately within the same region as the one found in a very fundamental empirical test.

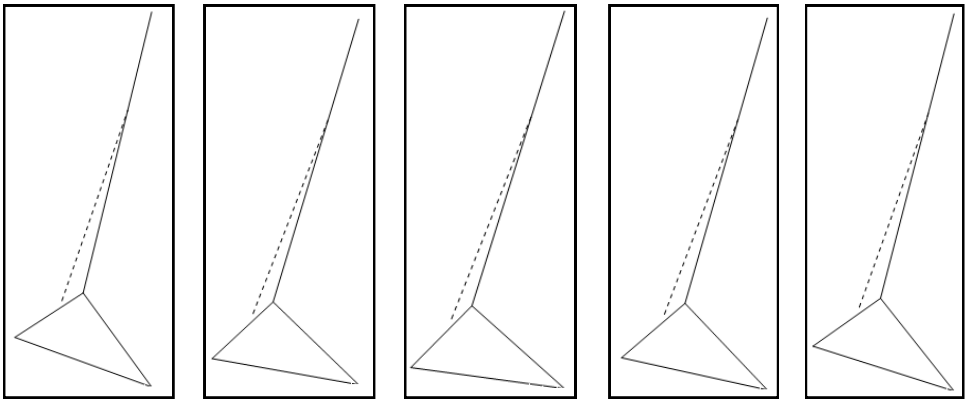

Figure 18: Schematic picture of the jump: Starting position at θ_{foot}=20.0° and θ_{ankle} =6.3°, lowest position at θ_{foot}=7.8° and θ_{ankle} =--9.7° and final position at θ_{foot}=19.7° and θ_{ankle} =6.0°

5.2.2 MT-unit

The most interesting results were the one for the MT-unit because it was primary this model that had been in focus during the model development. One of the aims of the MT-unit model was to make it working well with high velocity and large forces. It has been stated that under these conditions the passive structure gets a more important role and should be carefully modelled.

The figures below are showing the length of the whole MT-unit and the CE-unit respectively. The x-axis shows the time and the y-axis the actual length in metres.

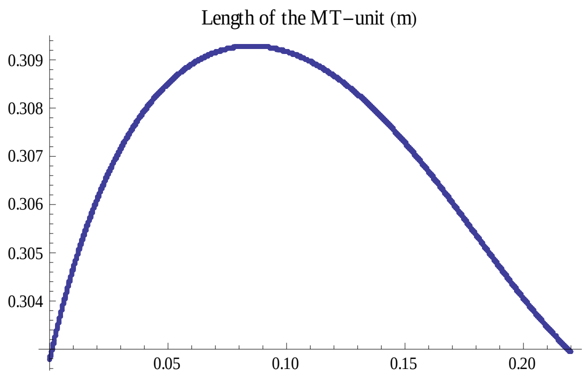

Figure 19: Length of MT-unit

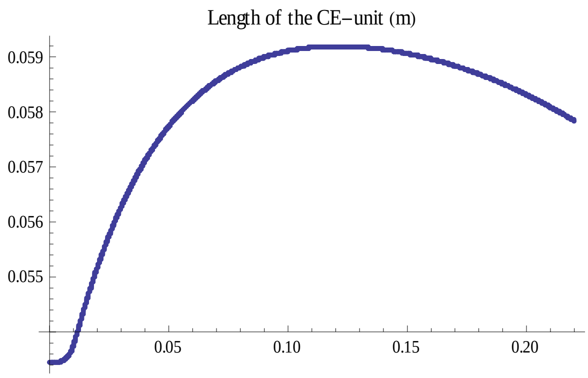

Figure 20: Length of CE-unit

The model consists of three tendons or tendon structures which are modelled as springs. Two of them are shown below. They are represented as the percentage of the tendon slack length. As can be seen, it begins with a fast lengthening followed by a slower shortening that is not linear.

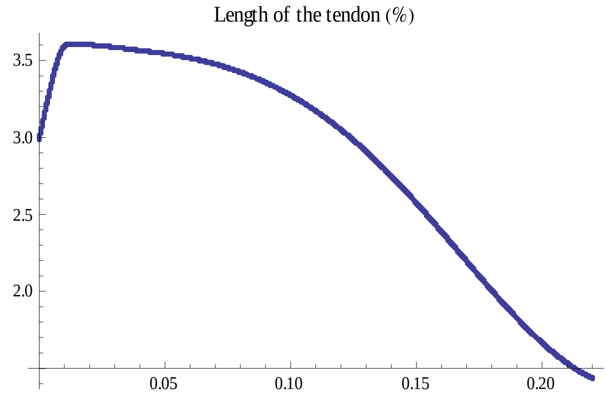

Figure 21: Elongation of tendon

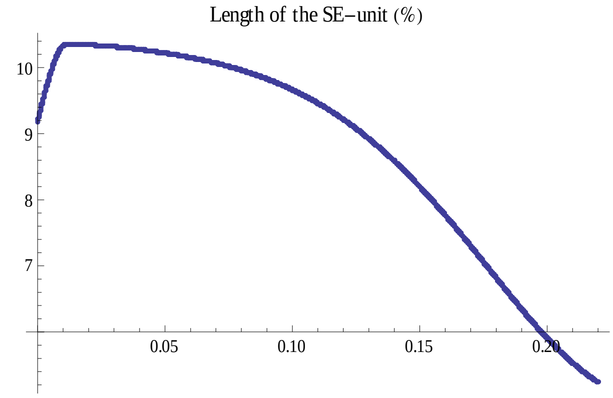

Figure 22: Elongation of SE-unit

When studying the graph for the force in the MT-unit (Figure 23) it can be seen that also here it is fast increase in the beginning followed by a decrease in force. The velocity, shown in Figure 24, clearly shows a very fast increase in the CE-unit which could be due to instability in the numerics in the beginning. The rest of the results seem to be realistic, so the fast increase in all the graphs should be used very carefully.

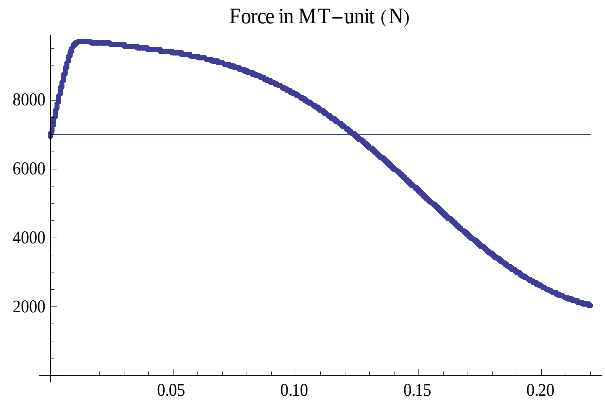

Figure 23: Force in MT-unit

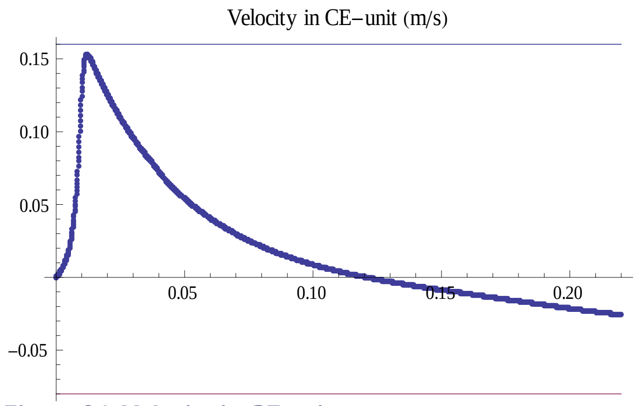

Figure 24: Velocity in CE-unit

6 Conclusions

This thesis has presented a new mathematical model of a musculotendon unit based on an old model. The model includes features for force-velocity and force-length relationship, elasticity of cross-bridges and the passive structures in muscles. The model is dimensionless which makes it possible to use for all skeletal muscles in the body together with the muscle specific parameters. Excluded in the model is the possibility of variable muscle activity and pennation angle. Running the musculotendon unit model within a drop jump simulation generated realistic results.

The introduction part introduced many interesting questions about muscle forces, optimal movement pattern and changes in movement pattern due to injury. Within this thesis no answers to these questions have been revealed and due to the complexity of the questions it was not expected. Additionally, one question was asking if it is possible to answer the questions above using computer simulations. The answer, after conducting this thesis, would be that the questions can be answered using validated computer simulations.

Despite the other conclusions, the major conclusion must be that building a musculotendon and musculoskeletal model is both complex and time consuming. Remembering back to the days when the thesis started I can only remember the endless possibilities and how easy everything was going to run. Looking back after 10 month, summarising the thesis I got a more realistic but much more experienced view of model development.

7 References

Alexander, R. M. (1991). "Energy-saving mechanisms in walking and running." Journal of Experimental Biology **160**(1): 55-69.

Anderson, F. C. and M. G. Pandy (1993). "Storage and utilization of elastic strain-energy during jumping." Journal of Biomechanics **26**(12): 1413-1427.

Anderson, F. C. and M. G. Pandy (1999). "A Dynamic Optimization Solution for Vertical Jumping in Three Dimensions." Computer Methods in Biomechanics and Biomedical Engineering **2**(3): 201 - 231.

Anderson, F. C. and M. G. Pandy (2001). "Dynamic optimization of human walking." Journal of Biomechanical Engineering-Transactions of the Asme **123**(5): 381-390.

Blemker, S. S. and S. L. Delp (2005). "Three-dimensional representation of complex muscle architectures and geometries." Annals of Biomedical Engineering **33**(5): 661-673.

Bobbert, M. F. (2001). "Dependence of human squat jump performance on the series elastic compliance of the triceps surae: A simulation study." Journal of Experimental Biology **204**(3): 533-542.

Brand, R. A., D. R. Pedersen, et al. (1986). "THE SENSITIVITY OF MUSCLE FORCE PREDICTIONS TO CHANGES IN PHYSIOLOGICAL CROSS-SECTIONAL AREA." Journal of Biomechanics **19**(8): 589-596.

Bullimore, S. R. and J. F. Burn (2007). "Ability of the planar spring-mass model to predict mechanical parameters in running humans." Journal of Theoretical Biology **248**(4): 686-695.

Cavagna, G. A. (2006). "The landing-take-off asymmetry in human running." Journal of Experimental Biology **209**(20): 4051-4060.

Cheng, K. B. and M. Hubbard (2004). "Optimal jumping strategies from compliant surfaces: A simple model of springboard standing jumps." Human Movement Science **23**(1): 35-48.

Cheng, K. Y. B. and M. Hubbard (2005). "Optimal compliant-surface jumping: a multi-segment model of springboard standing jumps." Journal of Biomechanics **38**(9): 1822-1829.

Cole, G. K., A. J. van den Bogert, et al. (1996). "Modelling of force production in skeletal muscle undergoing stretch." Journal of Biomechanics **29**(8): 1091-1104.

Damsgaard, M., J. Rasmussen, et al. (2006). "Analysis of musculoskeletal systems in the AnyBody Modeling System." Simulation Modelling Practice and Theory **14**(8): 1100-1111.

Davoodi, R., I. E. Brown, et al. (2003). "Advanced modeling environment for developing and testing FES control systems." Medical Engineering & Physics **25**(1): 3-9.

Delp, S. L. (1990). Surgery simulation: A computer graphics system to analyze and design musculoskeletal reconstructions of the lower limb. Department of Mechanical Engineering. Stanford, Stanford University. **Ph.D.:** 132.

Delp, S. L., F. C. Anderson, et al. (2007). "OpenSim: open-source software to create and analyze dynamic Simulations of movement." IEEE Transactions on Biomedical Engineering **54**(11): 1940-1950.

Delp, S. L. and J. P. Loan (1995). "A Graphics-based Software system to develop and analyze models of musculoskeletal structures." Computers in Biology and Medicine **25**(1): 21-34.

Eberhard, P., T. Spägele, et al. (1999). "Investigations for the dynamical analysis of human motion." Multibody System Dynamics **3**(1): 1-20.

Erdemir, A., S. McLean, et al. (2007). "Model-based estimation of muscle forces exerted during movements." Clinical Biomechanics **22**(2): 131-154.

Fernandez, J. W. and M. G. Pandy (2006). "Integrating modelling and experiments to assess dynamic musculoskeletal function in humans." Experimental Physiology **91**(2): 371-382.

Glitsch, U. and W. Baumann (1997). "The three-dimensional determination of internal loads in the lower extremity." Journal of Biomechanics **30**(11-12): 1123-1131.

Gregor, R. J., R. R. Roy, et al. (1988). "Mechanical output of the cat soleus during treadmill locomotion - in vivo vs in situ characteristics." Journal of Biomechanics **21**(9): 721-732.

Hall, S. J. (2003). Basic Biomechanics. Delaware, McGraw-Hill.

Hof, A. L. (2003). "Muscle mechanics and neuromuscular control." Journal of Biomechanics **36**: 1031–1038.

Huxley, A. F. (1974). "Muscular contraction." J Physiol **243**(1): 1-43.

Komi, P. V. (2000). "Stretch-shortening cycle: a powerful model to study normal and fatigued muscle." Journal of Biomechanics **33**(10): 1197-1206.

Marieb, E. N. (2004). Human Anatomy & Physiology. San Francisco, Daryl Fox.

Nagano, A., T. Komura, et al. (2005). "Force, work and power output of lower limb muscles during human maximal-effort countermovement jumping." Journal of Electromyography and Kinesiology **15**(4): 367-376.

Nagano, A., B. R. Umberger, et al. (2005). "Neuromusculoskeletal computer modeling and simulation of upright, straight-legged, bipedal locomotion of Australopithecus afarensis (AL 288-1)." American Journal of Physical Anthropology **126**(1): 2-13.

Pandy, M. G. (2001). "Computer modeling and simulation of human movement." Annual Review of Biomedical Engineering **3**: 245-273.

Pandy, M. G. (2003). "Simple and complex models for studying muscle function in walking." Philosophical Transactions of the Royal Society of London Series B-Biological Sciences **358**(1437): 1501-1509.

Pandy, M. G. and F. E. Zajac (1991). "Optimal muscular coordination strategies for jumping." Journal of Biomechanics **24**(1): 1-10.

Pandy, M. G., F. E. Zajac, et al. (1990). "An optimal-control model for maximum-height human jumping." Journal of Biomechanics **23**(12): 1185-1198.

Redl, C., M. Gfoehler, et al. (2007). "Sensitivity of muscle force estimates to variations in muscle-tendon properties." Human Movement Science **26**(2): 306-319.

Robilliard, J. J. and A. M. Wilson (2005). "Prediction of kinetics and kinematics of running animals using an analytical approximation to the planar spring-mass system." Journal of Experimental Biology **208**(23): 4377-4389.

Stålbom, M., D. J. Holm, et al. (2007). "Reliability of kinematics and kinetics associated with Horizontal Single leg drop jump assessment. A brief report." Journal of Sports Science and Medicine **6**(2): 261-264.

Thelen, D. G. (2003). "Adjustment of muscle mechanics model parameters to simulate dynamic contractions in older adults." Journal of Biomechanical Engineering-Transactions of the Asme **125**(1): 70-77.

Viceconti, M., D. Testi, et al. (2006). Biomechanics modeling of the musculoskeletal apparatus: Status and key issues. Proceedings of the IEEE.

Winters, J. M. and S. L. Y. Woo (1990). Multiple muscle systems : biomechanics and movement organization. New York, Springer-Verlag.

Zajac, F. E., R. R. Neptune, et al. (2002). "Biomechanics and muscle coordination of human walking - Part I: Introduction to concepts, power transfer, dynamics and simulations." Gait & Posture **16**(3): 215-232.

Zajac, F. E., R. R. Neptune, et al. (2003). "Biomechanics and muscle coordination of human walking - Part II: Lessons from dynamical simulations and clinical implications." Gait & Posture **17**(1): 1-17.

Zajac, F. E., E. L. Topp, et al. (1986). Musculotendon actuator models for use in computer studies and design of neuromuscular stimulation systems. RESNA '86, Minneapolis, MN, USA, Association for the Advancement of Rehabilitation Technology.

Appendix 1: Mathematica code

MT-unit - values and equations

```
Remove["Global`*"]

ak = 1;
```

- Soleus interface

```
F_IsoMax = 4000 + 3000;
l_Mopt = 0.08;
l_T0 = 0.22;
```

- Interface MS-model to MT model

$$\lambda_{T0} = \frac{l_{T0}}{l_{Mopt}};$$

- Starting configuration values

```
αS = 10^-12;
tsStart = 0;
dts = 10^-1;
tsEnd = 45 dts;
```

- Dynamic configurations values

```
dt = 10^-4;
tEnd = 0.22;

α = 10^-10;
tStart = 0;
NoTS = tEnd/dt;
```

Equations

- Fundamental eq.

```
PEEpoints = {{1, 0}, {1.3, 1}, {1.2, 0.5}};
PEEfit = Fit[PEEpoints, {1, λ_PE, λ_PE^2}, λ_PE];

λ_SE0 = 0.260567;
SEE1 = Solve[-1/10 + Q_1 e^(100 λ_SE) == 1 /. λ_SE → 0.284546] // Last;
Q_1 = Q_1 /. SEE1;

CEL1 = -0.418806 + 3.9661733996344957 Lλ_CE - 2.7717883853211207 Lλ_CE^2;
Plot[CEL1, {Lλ_CE, 0, 1.4}]
FindMaximum[CEL1, {Lλ_CE, 0.4}];
arne = FindRoot[CEL1 == 0, {Lλ_CE, 0.2}];
arne123 = FindRoot[CEL1 == 0, {Lλ_CE, 1.2}];
λ_CEmin = Lλ_CE /. arne
λ_CEmax = Lλ_CE /. arne123
```

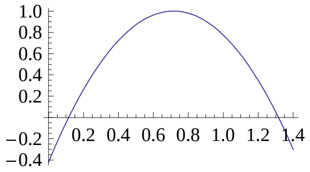

$$\mathtt{datavel} = \{\{-2, 0\}, \{0, 1\}, \{2.5, 1.4\}, \{-0.2, 0.5\}\};$$

$$\mathtt{kalle} = \mathtt{FindFit}\left[\mathtt{datavel},\ a + \frac{\mathrm{ArcTan}[b + c\, v_{CE}]}{d},\ \{a, b, c, d\},\ v_{CE}\right];$$

$$\begin{pmatrix} a \\ b \\ c \\ d \end{pmatrix} = \begin{pmatrix} a \\ b \\ c \\ d \end{pmatrix} \ /.\ \mathtt{kalle};$$

$$\mathtt{Tpoints} = \{\{0, 0\}, \{0.03, 1\}, \{0.02, 0.5\}\};$$

$$\mathtt{tenfit} = \mathtt{Fit}\left[\mathtt{Tpoints},\ \left\{1, \epsilon, \epsilon^2\right\},\ \epsilon\right];$$

$$\epsilon := (\lambda_T - \lambda_{T0}) / \lambda_{T0}$$

- Force equations

$$F_{PE} := \mathtt{If}[\lambda_{PE} > 1,\ \mathtt{PEEfit},\ 0]$$

$$F_{SE} := \mathtt{If}\left[\lambda_{SE} \geq \lambda_{SE0},\ -\frac{1}{10} + Q_1\, e^{100\,\lambda_{SE}},\ 10^{-3}\right]$$

$$F_{CEL} := \mathtt{If}\left[\lambda_{CEmin} < \lambda_{CE} < \lambda_{CEmax},\ \mathtt{CEL1}\ /.\ L\lambda_{CE} \to \lambda_{CE},\ 10^{-3}\right]$$

$$F_{CEV} := \mathtt{If}\left[-2 < v_{CE} < 2.5,\ a + \frac{\mathrm{ArcTan}[b + c\, v_{CE}]}{d},\ 0\right]$$

$$F_{CE} := F_{CEV}\, F_{CEL}\, ak$$

$$F_T := \mathtt{If}\left[\epsilon \geq 0,\ \frac{25}{3}\epsilon + \frac{2500}{3}\epsilon^2,\ 10^{-5}\right]$$

$$F_M := F_{CE} + F_{PE}$$

- Length equations

$$\lambda_{PE} := \lambda_M$$

Pre- simulation

The input values

```
g = 9.81;
θ1 start = 54; (* degrees *)
StartV = 0.27 √9.81 ;
dt = 0.0001;
ContactTime = 0.22;
```

- **Dimentions of the human simulated**

$$\text{Foot} = \begin{pmatrix} m_1 \\ l_{c1} \\ l_1 \\ J_1 \end{pmatrix} = \begin{pmatrix} 2.2 \\ 0.095 \\ 0.175 \\ 0.008 \end{pmatrix};$$

$$\text{Shank} = \begin{pmatrix} m_2 \\ l_{c2} \\ l_2 \\ J_2 \end{pmatrix} = \begin{pmatrix} 7.5 \\ 0.274 \\ 0.435 \\ 0.065 \end{pmatrix};$$

$$\text{Thigh} = \begin{pmatrix} m_3 \\ l_{c3} \\ l_3 \\ J_3 \end{pmatrix} = \begin{pmatrix} 15.15 \\ 0.251 \\ 0.400 \\ 0.126 \end{pmatrix};$$

$$\text{HAT} = \begin{pmatrix} m_4 \\ l_{c4} \\ l_4 \\ J_4 \end{pmatrix} = \begin{pmatrix} 51.22 \\ 0.343 \\ 0.343 \\ 6.814 \end{pmatrix};$$

The musculoskeletal model

θ_2 - position and acceleration

$$\text{Th2}[t\_] := \text{ArcCos}\left[-\frac{l_1}{l_2}\,\text{Cos}[\theta 1[t]]\right]$$

$$\text{Hdd}\theta_2 := \text{D}[\text{Th2}[t], \{t, 2\}]$$

$$\text{dd}\theta_2 = \text{Hdd}\theta_2 \;/.\; \{\theta 1[t] \to \theta_1,\ \theta 1'[t] \to \text{d}\theta_1,\ \theta 1''[t] \to \text{dd}\theta_1\};$$

Positions

$$y_{fot}[t\_] := l_{c1}\,\text{Sin}[\theta 1[t]]$$
$$y_{underben}[t\_] := l_1\,\text{Sin}[\theta 1[t]] + l_{c2}\,\text{Sin}[\text{Th2}[t]]$$
$$x_{underben}[t\_] := l_1\,\text{Cos}[\theta 1[t]] + l_{c2}\,\text{Cos}[\text{Th2}[t]]$$
$$y_{knä}[t\_] := l_1\,\text{Sin}[\theta 1[t]] + l_2\,\text{Sin}[\text{Th2}[t]]$$

Velocities

$$v_{underben} = \text{D}[y_{underben}[t], t];$$
$$v_{underbenX} = \text{D}[x_{underben}[t], t];$$
$$v_{knä} = \text{D}[y_{knä}[t], t];$$

Kinetic energy

$T_{TOT} := T_{rot1} + T_{rot2} + T_{trans2y} + T_{trans2x} + T_{trans2yk}$

$T_{rot1} = \frac{1}{2}\left(J_1 + m_1\, l_{c1}{}^2\right)(\theta 1'[t])^2;$

$T_{rot2} = \frac{1}{2}(J_2)(Th2'[t])^2;$

$T_{trans2y} = \frac{1}{2} m_2 (v_{underben})^2;$

$T_{trans2x} = \frac{1}{2} m_2 (v_{underbenX})^2;$

$T_{trans2yk} = \frac{1}{2} (m_3 + m_4) (v_{knä})^2;$

Potential energy

$Moment := F_{SOL}\, r_{MT}$

$V_{TOT} = m_1\, g\, y_{fot}[t] + m_2\, g\, y_{underben}[t] + (m_3 + m_4)\, g\, y_{knä}[t] + 2\, Moment\, Th2[t];$

Lagrangian

$L := T_{TOT} - V_{TOT}$

$L_{EjT} = L /. \{\theta 1[t] \to \theta_1, \theta 1'[t] \to d\theta_1\};$

$der1 = D[L_{EjT}, d\theta_1];$
$der12 = D[L_{EjT}, \theta_1];$

$der112 = der12 /. \{\theta_1 \to \theta 1[t], d\theta_1 \to \theta 1'[t]\};$

$MomFor1 = D[der1 /. \{\theta_1 \to \theta 1[t], d\theta_1 \to \theta 1'[t]\}, t] - der112;$
$MomFor1 /. \{\theta 1[t] \to \theta_1, \theta 1'[t] \to d\theta_1\};$

$MomEkv1 = Solve[MomFor1 == 0, \theta 1''[t]] // Last;$
$Tempdd\theta = \theta 1''[t] /. MomEkv1;$
$dd\theta_1 := Tempdd\theta /. \{\theta 1[t] \to \theta_1, \theta 1'[t] \to d\theta_1\}$

Drop jump input equations

- **Calcutation momentarm for soleus**

```
momentarm = Import["soleus_momentarm_calc.txt", "Table"];
momentarm[[All, 1]] = momentarm[[All, 1]];
func = Fit[momentarm, {1, ma, ma^2}, ma]
Show[Plot[func, {ma, -50, 40}], ListPlot[momentarm]]
```

$-0.0413893 + 0.000236548\, ma + 5.55314 \times 10^{-6}\, ma^2$

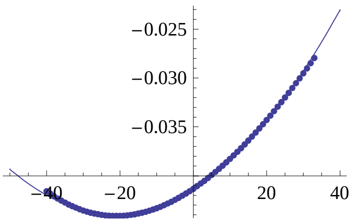


```
ma := AnkleAngle
```

$r_{MT} := -func$

- **Equations**

Transformation equations

$$DtR = \frac{\pi}{180};$$

$$RtD = \frac{180}{\pi};$$

MT-unit length

$$LMTL = 0.65;$$

$$CMTA = \frac{\pi}{18};$$

$$FMTF = 1.07;$$

$$l_{MT} := \sqrt{\left((l_1 \text{Cos}[\theta_1] + LMTL\, l_2 \text{Cos}[\theta_2] - FMTF\, l_1 \text{Cos}[\theta_1 - CMTA])^2 + (l_1 \text{Sin}[\theta_1] + LMTL\, l_2 \text{Sin}[\theta_2] - FMTF\, l_1 \text{Sin}[\theta_1 - CMTA])^2\right)}$$

Starting values

```
brossan = D[l1 Cos[θ1[t]] + l2 Cos[θ2[t]], t];
kossan = D[l1 Sin[θ1[t]] + l2 Sin[θ2[t]], t];
ekv400 = Solve[{brossan == 0, kossan == -StartV}, {θ1'[t], θ2'[t]}] // Last;
```

```
dθ1 := θ1'[t] /. ekv400 /. {θ1[t] → θ1, θ2[t] → θ2}
dθ2 := θ2'[t] /. ekv400 /. {θ1[t] → θ1, θ2[t] → θ2}
```

$$\theta_1 = \theta_{1\,start}\, DtR;$$

$$\theta_2 := \text{ArcCos}\left[-\frac{l_1}{l_2} \text{Cos}[\theta_1]\right];$$

Joint angles

```
FootAngle := θ1 RtD - 34
AnkleAngle := θ1 RtD - 34 + 90 - θ2 RtD
```

Starting configuration

```
λ_MT := l_MT / l_Mopt

v_CEStart = 0;
i = 0;

λ_M := λ_MT - λ_T

For[t = tsStart; is = 0, t ≤ tsEnd, t = t + dts,
 (* Equation for length change of MT *)
 λ_MT;

 (* Finding F_T = F_M with λ_T *)
 λ_TG = If[is < 1, λ_T0, λ_T];
 λ_T = If[is < 1, λ_T0 + 2 αS, λ_T + 2 αS];
 While[Abs[λ_T - λ_TG] > αS,
  (* Calculation of mean *)
  λ_T = (λ_TG + λ_T)/2;
  (* Updates λ *)
  λ_M; λ_PE;

  (* Calculates λ_SE *)
  λ_SEG = If[is < 1, λ_SE0, λ_SE];
  λ_SE = If[is < 1, λ_SE0 + 2 αS, λ_SE + 2 αS];

  While[Abs[λ_SE - λ_SEG] > αS,
   (* Calculation of mean *)
   λ_SE = (λ_SEG + λ_SE)/2;
   (* λ_CE & v_CE *)
   λ_CE = λ_M - λ_SE;
   v_CE = If[is < 1, v_CEStart, (λ_CE - λ_CEFT)/dts];
   (* Calculates new λ_SE *)
   F_CEL; F_CEV;
   F_SEN = F_CEV F_CEL ak;
   ekv1 = FindRoot[-1/10 + Q_1 e^(100 λ_SEF) == F_SEN, {λ_SEF, λ_SE0}];
   λ_SEG = λ_SE;
   λ_SE = λ_SEF /. ekv1;
  ];

  (* Calculating F_M *)
  F_PE; F_SE;
  F_TN = F_PE + F_SE;
  ekv2 = FindRoot[25/3 ((λ_TF - λ_T0)/λ_T0) + 2500/3 ((λ_TF - λ_T0)/λ_T0)^2 == F_TN, {λ_TF, 1.5 λ_T0}];
  λ_TG = λ_T;
  λ_T = λ_TF /. ekv2;
 ];
```

```
λCEFT = λCE;
FT;
is = is + 1;
]
```

- **Preparation for the dynamic cofiguration**

```
λCEStart = λCE

λCE = λCEStart;
vCE = 0;
λT := λMT - λM
```

- **Tables for evaluation of the dynamic configuration**

```
ItTot = 0;
Kont1 = Table[0, {40 000}, {2}];
```

$$Kont2 = Table\left[0, \left\{\frac{ContactTime - 0}{dt} + 1\right\}, \{2\}\right];$$

$$NForceSE = Table\left[0, \left\{\frac{ContactTime - 0}{dt} + 1\right\}, \{2\}\right];$$

$$NForceCE = Table\left[0, \left\{\frac{ContactTime - 0}{dt} + 1\right\}, \{2\}\right];$$

$$NForcePE = Table\left[0, \left\{\frac{ContactTime - 0}{dt} + 1\right\}, \{2\}\right];$$

$$NForceT = Table\left[0, \left\{\frac{ContactTime - 0}{dt} + 1\right\}, \{2\}\right];$$

$$NForceM = Table\left[0, \left\{\frac{ContactTime - 0}{dt} + 1\right\}, \{2\}\right];$$

$$NLengthSE = Table\left[0, \left\{\frac{ContactTime - 0}{dt} + 1\right\}, \{2\}\right];$$

$$NLengthCE = Table\left[0, \left\{\frac{ContactTime - 0}{dt} + 1\right\}, \{2\}\right];$$

$$NLengthT = Table\left[0, \left\{\frac{ContactTime - 0}{dt} + 1\right\}, \{2\}\right];$$

$$NLengthM = Table\left[0, \left\{\frac{ContactTime - 0}{dt} + 1\right\}, \{2\}\right];$$

$$NLengthMT = Table\left[0, \left\{\frac{ContactTime - 0}{dt} + 1\right\}, \{2\}\right];$$

$$ContFCE = Table\left[0, \left\{\frac{ContactTime - 0}{dt} + 1\right\}, \{2\}\right];$$

$$ContSECE = Table\left[0, \left\{\frac{ContactTime - 0}{dt} + 1\right\}, \{2\}\right]; NVelCE = Table\left[0, \left\{\frac{ContactTime - 0}{dt} + 1\right\}, \{2\}\right];$$

Dynamic configuration code

```
For[tt = 0; iq = 0, tt ≤ ContactTime, tt = tt + dt,
 (* Updates momentarm soleus *)
 ma; r_MT;
 (* Updates MT-unit length *)
 l_MT;

 (*------------------------ The MT-Unit model ------------------------------*)
 λ_MT;
 (* Equation for length change of MT *)
 λ_CE = λ_CE + v_CE dt;
 If[λ_CE < λ_CEmin, λ_CE = λ_CEmin];

 (* Finding F_T = F_M with λ_SE *)
 NrIt1 = 0;
 λ_SEG = λ_SE;
 λ_SE = λ_SE + 2 α;

 While[Abs[λ_SE - λ_SEG] > α,
  (* Calculating mean *)
  λ_SE = (λ_SEG + λ_SE)/2;
  (* Updates λ *)
  λ_M = λ_SE + λ_CE;
  λ_T; λ_PE;

  F_SEB = F_T - F_PE;
  If[F_SEB < 10^-6, λ_SE, ekv2 = FindRoot[-1/10 + Q_1 e^(100 λ_SEF) == F_SEB, {λ_SEF, 1.5 λ_SE0}]];
  If[F_SEB < 10^-6, λ_SEG = λ_SE, λ_SEG = λ_SE; λ_SE = λ_SEF /. ekv2];
  (* Calculates λ_T *)

  ItTot = ItTot + 1;
  NrIt1 = NrIt1 + 1;
  Kont1[[ItTot, 2]] = λ_T;  Kont1[[ItTot, 1]] = ItTot;
 ];

 (* Calculating new velocity *)
 F_CEL;
 F_CEB = F_SE/(F_CEL ak);
 ekv10 = FindRoot[F_CEB == a + ArcTan[b + c v_CEF]/d, {v_CEF, 0}];
 v_CE = v_CEF /. ekv10;
 If[v_CE < -20, v_CE = -2, If[v_CE > 20.5, v_CE = 2.5, v_CE]];

 (* Saving data into tables *)
 i = i + 1;
 Kont2[[i, 2]] = NrIt1;    Kont2[[i, 1]] = tt;

 NForceSE[[i, 2]] = F_SE;     NForceSE[[i, 1]] = tt;
 NForceCE[[i, 2]] = F_CE;     NForceCE[[i, 1]] = tt;
```

```
NForcePE[[i, 2]] = F_PE;    NForcePE[[i, 1]] = tt;
NForceT[[i, 2]] = F_T;      NForceT[[i, 1]] = tt;
NForceM[[i, 2]] = F_M;      NForceM[[i, 1]] = tt;

NLengthSE[[i, 2]] = λ_SE;      NLengthSE[[i, 1]] = tt;
NLengthCE[[i, 2]] = λ_CE;      NLengthCE[[i, 1]] = tt;
NLengthT[[i, 2]] = λ_T;        NLengthT[[i, 1]] = tt;
NLengthM[[i, 2]] = λ_M;        NLengthM[[i, 1]] = tt;
NLengthMT[[i, 2]] = λ_MT;      NLengthMT[[i, 1]] = tt;

ContFCE[[i, 2]] = F_CEB;       ContFCE[[i, 1]] = tt;
ContSECE[[i, 2]] = λ_SE + λ_CE;  ContSECE[[i, 1]] = tt;

NVelCE[[i, 2]] = v_CE;    NVelCE[[i, 1]] = tt;
F_SOL = F_M * F_IsoMax;
(*-------------------- END MT-Unit model ------------------------*)

(* Joint torque *)
Moment;
(* Calculating new acc *)
ddθ1;
ddθ2;
(* Updates variables*)
θ1 = θ1 + dθ1 dt + (ddθ1 dt^2)/2;
dθ1 = dθ1 + ddθ1 dt;
θ2; dθ2;


(* Saving results into tables *)
iq = iq + 1;
Thh1[[iq, 2]] = θ1;    Thh1[[iq, 1]] = tt;
Thh2[[iq, 2]] = θ2;    Thh2[[iq, 1]] = tt;
dTh1[[iq, 2]] = dθ1;  dTh1[[iq, 1]] = tt;
dTh2[[iq, 2]] = dθ2;  dTh2[[iq, 1]] = tt;
MuscleL[[iq, 2]] = l_MT;  MuscleL[[iq, 1]] = tt;
momarm[[iq, 2]] = r_MT;  momarm[[iq, 1]] = tt;
Fotredo[[iq, 2]] = FootAngle;  Fotredo[[iq, 1]] = tt;
Ankelredo[[iq, 2]] = AnkleAngle;  Ankelredo[[iq, 1]] = tt;
]
```